Inorganic Chemistry

pubs.acs.org/IC

Article

Coordination of PPh_3 with a $[Mo_2O_2(\mu\text{-}S)_2]^{2+}$ Phosphinoyldithioformate Complex and Its Influence on Episulfide Sulfur Abstraction

Dmitrii Razinkov, Ágúst Kvaran, Sigridur Jonsdottir, and Sigridur G. Suman*

Cite This: *Inorg. Chem.* 2025, 64, 4431−4446

Read Online

ACCESS | Metrics & More | Article Recommendations | Supporting Information

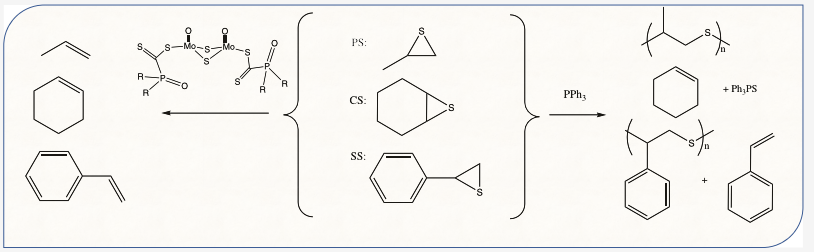

ABSTRACT: Phosphinoyldithioformate ligands in binuclear molybdenum−sulfur complexes offer a synergistic environment for sulfur transfer (SAT) reactions. Relevant complex, **3**, and its SCN^- derivative, **4**, as two salts **4a** and **4b** were formed. Reactions of **3**, and **4b** with cyclohexene sulfide (CS), styrene sulfide (SS), and propylene sulfide (PS) were studied. Different stabilities of **3** and **4b**, as **4b** > **3**, allowed comparisons of reactivity based on the ability of the ligands to accommodate the episulfides. A moderate reactivity of CS, SS, and PS with **3** was arranged as CS > SS > PS, while its reactivity with **4b** was negligible. The addition of PPh_3 was found to increase the rate of reaction of **3** with CS to form Ph_3PS. PPh_3 reacted with SS and PS, to form Ph_3PS and polythioether as SS < PS. PPh_3 reacts with **3** to abstract a sulfur atom. The mechanism of the SAT reaction is proposed to take place in two steps to form a sulfurated complex followed by ~~its~~ sulfur expulsion, while the addition of PPh_3 replaces the expulsion step with a faster Ph_3PS formation. **3** was ascertained as an efficient catalyst and the nonrigid ligands accommodated the episulfides and PPh_3 in their reactions without evident catalyst deactivation.

INTRODUCTION

Sulfur atom transfer (SAT) reaction is a key reaction in many substitution reactions of thiolate complexes employed for hydrodesulfurization (HDS),[1−3] model reactions of metalloenzymes,[4−6] or iron−sulfur proteins.[7,8] Sulfur atom transfer has many industrial applications and has, therefore, received extensive attention.[9−13] The rate and mechanism of H_2S elimination from a catalyst and the nature of the HDS active site are still debated.[1,13] By analogy, the reductive elimination of H_2S or thiols (RSH) from complexes could be very slow and, therefore, rate-determining. The direct metal-mediated SAT reactions employing molybdenum,[14−21] tungsten,[22−25] rhenium,[26] or rhodium,[27−30] complexes have been reported, where mononuclear complexes undergo facile oxidative addition of sulfur or thiolate and reductive elimination in a catalytic reaction.[14,22] A major drawback identified involves catalyst deactivation through dimerization of the catalyst. Certain characteristics have been highlighted that may improve catalyst performance through improved catalyst stability and efficiency.[14,22] Sulfur atom transfer from an episulfide to a metal may proceed through either an oxidative addition to the metal or in a ligand-based insertion redox reaction into M−S bonds.[11,12,31,32] Bulky phosphine ligands may prevent common obstacles like dimerization and subsequent deactivation of the catalyst.[14,33] Dinuclear molybdenum sulfur complexes have a natural ability to coordinate sulfur and add sulfur atoms into terminal Mo−S bonds to form sulfur ligands with several sulfur atoms.[34] These sulfur ligands undergo an internal redox reaction where elemental sulfur is expelled when the ring size becomes sterically crowded.[34] PPh_3 is well-known to react rapidly with available sulfur or oxygen in Mo and W complexes,[26,35−39] where the addition of PPh_3 to a catalytic reaction significantly increased the apparent SAT reaction rates.[26,35] PPh_3 reacts spontaneously with sulfur, albeit sufficiently slowly, to negligibly impact its reaction with sulfur in the complex.

Ambidentate phosphinoyldithioformate ligands have been shown to adapt versatile coordination preferences that depend on the Lewis acidity of the metal center and on the steric and

Received: December 4, 2024
Revised: February 11, 2025
Accepted: February 13, 2025
Published: February 25, 2025

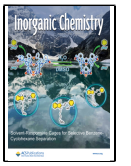

electronic properties imparted by the substituent on the phosphorus atom.[40−42] These substituents also influence the physical properties of the compounds, such as solubility and crystallinity. Compounds of phosphinoyldithioformate ligands with the $[Mo_2O_2(\mu\text{-}S)_2]^{2+}$ core were found to exhibit nonrigid behavior in solution while adopting octahedral geometry around the Mo centers.[43] Despite coordinative saturation, the Mo centers proved to be able to catalytically remove sulfur atoms from activated episulfides. A bimetallic mechanism was proposed where the sulfur is inserted into a metal−sulfur bond releasing the alkene followed by sulfur expulsion.[43] A mechanism proposed for the $Mo(CO)_6$ desulfuration of episulfides similarly suggests the formation of a metallacycle.[44] The rate-determining step was found to be the sulfur expulsion step based on the identification of the triply bridged sulfur intermediate by ESI MS and also influenced by solvent properties.[43] To increase solubility and potential catalytic activity, a phenethyl-substituted phosphinoyldithioformate ligand, **2**, was synthesized, and its mixed ligand octahedral complexes with DMF (**3**), and SCN^- (**4**) were synthesized. The catalytic abilities of **3** and **4b** in SAT reactions were evaluated alone and in the presence of PPh_3. Importantly, **3** was found to be an effective catalyst without evident deactivation.

RESULTS AND DISCUSSION

Syntheses and Characterization. *Syntheses.* Ligand **1** was prepared by using a Grignard reaction to obtain a new substituent on ligand **2** (Scheme 1). Me_4N[**2**], ligand **2,** was prepared by condensing **1** with CS_2, followed by a cation exchange. Complex **3** was synthesized in ligand exchange reactions of Me_4N[**2**] with $(Me_4N)_2[Mo_2O_2(\mu\text{-}S)_2(Cl)_4]$,[45] in DMF at aerobic conditions and room temperatures (Scheme 1). Complex **3** further reacted with two equivalents of $(Et_4N)SCN$ or $(Bu_4N)SCN$ in DMF at ambient temperature to form **4a** and **4b.**

Scheme 1. Synthesis of Compounds

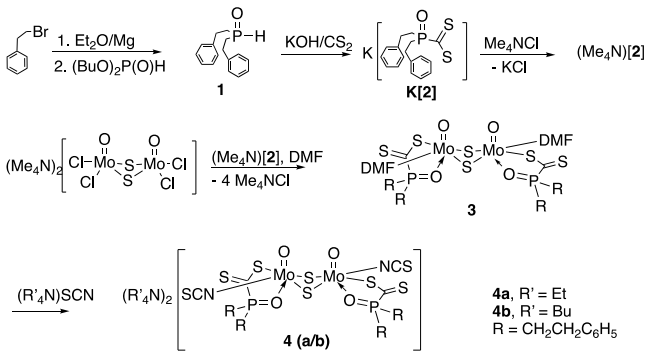

Employing a Grignard reaction described here results in a 76% yield of **1**.[46] Several syntheses of **1** were previously reported from a reaction of styrene with various forms of phosphorus in the superbasic KOH-DMSO system resulting in partial oxidation of the secondary phosphine **1** to a tertiary phosphine side product.[47] Alternate reactions employing styrene with red or white phosphorus also form **1**, albeit in much lower yields.[47,48] The tertiary phosphine side product was not observed in the Grignard reaction, and the product was isolated as a crystalline solid. Scheme 1 depicts the synthetic routes for the compounds, with details given in the experimental section. The reactions to form **3** and **4** were conducted in stoichiometric ratios (Scheme 1).

The compounds **1**−**4** were characterized spectroscopically, by mass spectrometry and elemental analysis. **3**−**4** are microcrystalline dark red and orange solids that formed in good yields with moderate solubility in organic solvents. The salts of compound **2** are pink crystalline solids.

Two different salts of **4**, Et_4N^+ (**4a**) and Bu_4N^+ (**4b**) were synthesized and characterized to evaluate their nonrigid properties under the reaction conditions employed. Complexes **3** and **4b** were chosen for catalytic studies due to **4b** superior solubility to **4a** in nonpolar noncoordinating solvents.

Molecular Structure Analyses. A summary of crystal data and structural refinement parameters for K[**2**], and **4a** is given in Table S1. Selected bond distances and angles are given in Tables S2−S5.

X-ray quality single crystals of $K\{(PhCH_2CH_2)_2P(O)CS_2\}\text{-}(C_4H_8O_2)_{0.5}$, K[**2**] were obtained by diffusion of dioxane/ether (1:1) mixture into a THF solution (Figure 1a). The potassium cation revealed strong electrostatic interactions with the CS_2^- moiety when comparing the sum of the covalent radius of potassium and oxygen (2.59 Å), or sulfur (2.99 Å) atoms respectively, and the van der Waals radius for the same (4.27 Å/4.55 Å).[49] The *iso*-bidentate CS_2^- moiety for the C−S bonds was confirmed and is comparable to that reported for $(Ph_4P)\{Ph_2P(O)CS_2\}$ (Table S2).[42] This important characteristic of the CS_2^- moiety coordination is observable in the IR spectrum.[40] The P═O bond distance was found to be slightly long 1.500(2) Å compared to similar reported P═O bond distances and shorter than single P−O bond distances of 1.526 Å.[42,50−54]

Single crystals of **4a,** $(Et_4N)_2[Mo_2O_2(\mu\text{-}S)_2(\mathbf{2})_2(SCN)_2]$ were obtained by the slow evaporation of a saturated solution of **4a** in acetonitrile. Figure 1b shows the ellipsoidal plot of the chiral anion of **4a**.

The molecular Mo centers are related by a C_2 axis, and the anion plot was generated by symmetry. The NCS^-, isothiocyanato ligand, is linear with a 179.8° N−C−S angle. The equatorial position *trans* to each other is a common arrangement for monodentate ligands in this system.[43,55−59] The Mo−N bond distance is 2.178(17) Å and comparable to 2.174(5) Å obtained for the Mo−N bond distance in $[Mo_2O_2(\mu\text{-}S)_2(SCN)_5(CH_3CN)]^{3-}$.[60] Ligand **2** coordinates in an S,O-bidentate coordination mode with the sulfur donor atoms in the equatorial plane and the oxo donor *trans* to the molybdenyl group. This coordination mode of the phosphinoyldithioformate ligand results in a P═O bond distance of 1.503(18) Å compared to 1.500(17) Å in **2**, and 1.506(10) Å in $[Ph_2Pb\{Ph_2P(O)CS_2\}_2(H_2O)]$ and 1.519(19) Å in $[Mo_2O_2(\mu\text{-}S)_2\{Ph_2P(O)CS_2\}_2(DMF)_2]$.[40,43] The Mo−O1, and Mo−S1 bond distances are unexceptional.[43,60−62] Trans-influence of the molybdenyl group leads to an elongated Mo−O2 bond of 2.21(10) Å compared to the expected 1.95(10) Å for Mo−O single bond and in good agreement with reported values of 2.30(16) and 2.25(15) Å for $K_2[Mo_2O_2(\mu\text{-}S)_2(cys)_2]$ and $[Mo_2O_2(\mu\text{-}S)_2(DMF)_6]$ respectively.[45,60,63−66] The dihedral angle of the core $[Mo_2O_2(\mu\text{-}S)_2]^{2+}$ in **4a** was calculated as 160.4°, at the upper reported range of 150 to 160° for similar compounds.[43,60,61,67] The Mo−Mo distance was calculated as 2.842 Å or slightly longer than the 2.835 Å for $[Mo_2O_2(\mu\text{-}S)_2\{Ph_2P(O)CS_2\}_2(DMF)_2]$.[43] Compared to the structure of **2**, the C1−S bond distances are nonequidistant as expected for dithioformate with a single metal−sulfur bond (C−S dist., =

https://doi.org/10.1021/acs.inorgchem.4c05188
Inorg. Chem. 2025, 64, 4431−4446

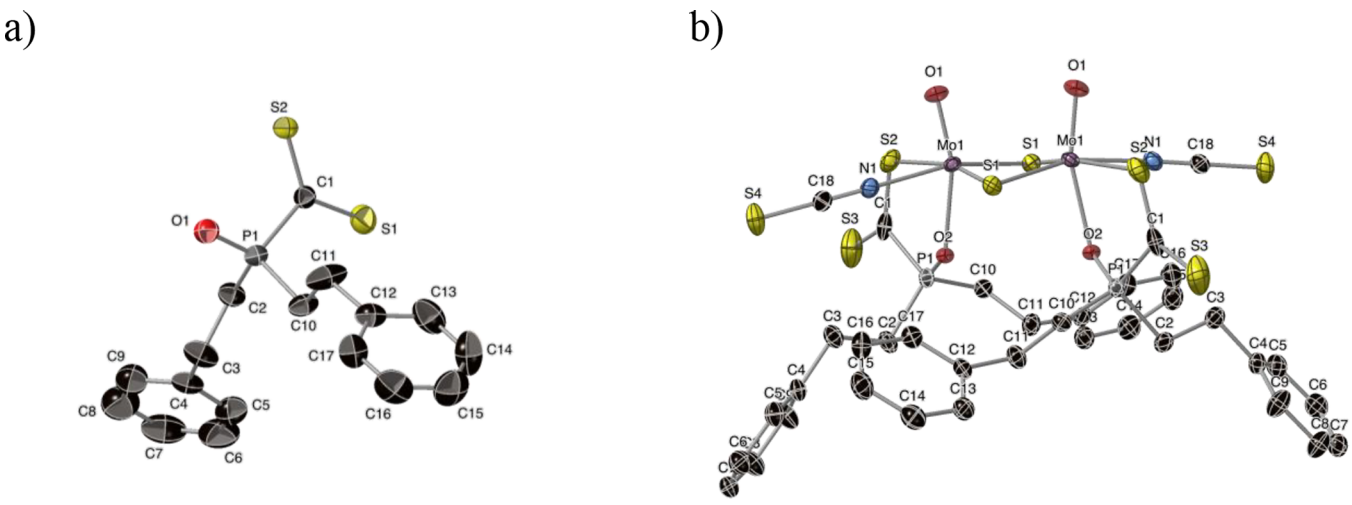

Figure 1. Molecular structure (a) depicting the atom labeling of **2**, and (b) Molecular structure of the anion of **4a.** Hydrogen atoms are omitted for clarity.

Table 1. Selected $^{13}C\{^1H\}$ and $^{31}P\{^1H\}$ NMR data [δ, ppm, J(Hz)] for 1−2 and 3−4[a]

comp.	PPh_3[b]	Ph_3PS[b]	1	(Me_4N)[2]	3	4a	4b
δ,$^{31}P\{^1H\}$	−5.3 (s)	43.3 (s)	31.0 (s)	43.8 (s)	80.1 (s, br.), 79.7 (s, br.)	65.9 (s)	66.6 (s)
δ(SCN),$^{13}C\{^1H\}$						142.8 (s)	143.8 (s)

[a]**2** in D_2O, **1, 3,** in $CDCl_3$, **4a** in DMSO-d_6, **4b** in $CDCl_3$. [b]*This work* in $CDCl_3$ and ref 68.

1.683(3) Å) and a C═S bond (1.650(3) Å), as reflected in the IR spectrum of **4a.**

Comparable dithioformate C−S bond distances in the S,O-bonded $[Ph_2Pb\{Ph_2P(O)CS_2\}_2(H_2O)]$ are 1.701(2), and 1.651(2).[40] The angle O1−Mo−O2 is 160.2°, and the N1−Mo−S2 angle is 77.2°, resulting in an overall distorted octahedral geometry around the Mo-center. Complex **3** is significantly more soluble than its phenyl or benzyl counterparts,[43] but the phenethyl substituents also impart steric bulk to the Mo centers as seen in the crystal structure (Figure 1b). This orientation with the O donor atom *trans* to the Mo═O group results in more steric hindrance than if the O donors were *cis* positioned, along with the prediction of increased lability caused by the *trans influence* of the molybdenyl group.

Chemical Characterization. The phosphinoyldithioformate ligands are ambidentate nonrigid ligands that may coordinate in many coordination modes as demonstrated for phenyl and benzyl substituted analogous complexes.[43] Analysis of **1−4** was performed using ^1H, $^{13}C\{^1H\}$ NMR, and $^{31}P\{^1H\}$ NMR spectroscopy, electronic spectroscopy, IR spectra, and elemental analysis. The NMR spectroscopic details for ligands and complexes are given in the experimental section and in Figures S7−S19. Atom labeling scheme is given for the ^1H and $^{13}C\{^1H\}$ NMR in Scheme S1. Mass spectrometry data was collected for the compounds **1−4**. Observed and simulated mass spectra and m/z values for **3** and **4a**/**b** are given in the SI (Figures S21−26) and the experimental.

Infrared spectra of the ligands **1−2** showed the expected vibrational bands for the ligand and complex functional groups (Figures S1−S3) consistent with previously reported data (see experimental).[40,43,46] The solid-state coordination of **2** is consistent with an S,O bidentate coordination in **3** and **4a**/**b** (Figures S4−S6) as confirmed by the crystal structure analysis of **4a**. In **4**, the isothiocyanato ligands were observed at an energy expected for N-coordinated SCN^- ligands.[60] Compounds **3** and **4** exhibit single major bands for the dithioformate and phosphinoyl groups in the IR spectra, as S,O bidentate chelate moieties shift to higher (C═S; *aniso*-CS_2^-), and lower energy weak C−S stretch (see experimental). The solution IR spectrum of **4b** in $CHCl_3$ confirmed that the S,O-bidentate coordination is present in solution, as well. The ^1H NMR spectra of bis(phenylethyl)phosphine oxide, **1**, potassium, and tetramethylammonium salts of **2** revealed two multiplet signals for α-methylene protons and a single multiplet for β-methylene protons. The protons on the two phenyl groups on each ligand were observed as two multiplet signals with overlapping *ortho*, *meta*, and *para* protons. Obtained spectra of **1−4** revealed that the two phenethyl groups on phosphorus are not chemically equivalent.

The ^1H NMR spectra for **3−4a**/**b** at ambient temperature show a single set of protons for the ligands, and the DMF is dissociated in solution. Integration of the resonances in all spectra gave satisfactory results, although the signals for **3−4a**/**b** are broad and only partially resolved. Data and coupling constants for the $^{13}C\{^1H\}$ NMR spectra are given in the experimental section. The dithioformate group was observed as a doublet for the C^7 atom (Scheme S1). Phosphorus couples to carbon over three bonds in **1−4**, revealing doublets for α-/β-methylene carbons (C^1, C^2) and *ipso*-carbons (C^3), and singlets for the *ortho*-, *meta*- and *para*-carbons (C^4, C^5, C^6) of **1−4**. Table 1 provides the N-coordinated SCN^- carbon atom chemical shifts for **4a**/**b**, and the phosphorus atom chemical shifts for **1−4**. The $^{31}P\{^1H\}$ NMR spectra of **3**, **4a,** and **4b** (Figure S13) at ambient temperature are given in Table 1 and Figure S13.

Based on crystal structure analysis of both **4a** and $[\{Ph_2P(O)CS_2\}_2Mo_2O_2(\mu\text{-}S)_2(DMF)_2]$, the Mo−S and Mo−O(ligand) bonds favor the *cis* and *trans* positions to the Mo═O group respectively, leaving *cis* coordination for the DMF ligands and a single signal in the $^{31}P\{^1H\}$ NMR spectrum for

https://doi.org/10.1021/acs.inorgchem.4c05188
Inorg. Chem. 2025, 64, 4431−4446

Scheme 2. $^{31}P\{^{1}H\}$ NMR Chemical Shifts of Coordination Isomers of **3** in DMF-d_7[a]

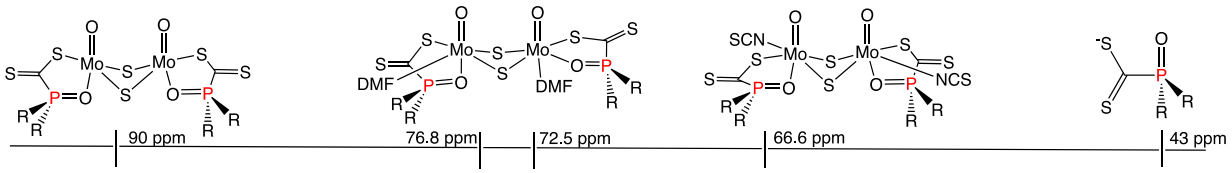

[a] **4b** and **2** are shown for comparison.

4a and **4b**.[43] The $^{31}P\{^{1}H\}$ NMR spectrum of **3** results in two P signals for the mixed *cis*/*trans* coordination of the ligand O-donor and DMF (Scheme 2).[43] Upon dissociation of DMF, a downfield shift of the P signal was observed at 90 ppm.

Comparison of reported data reveals a downfield shift of about 10 to 15 ppm of the P signal in the $^{31}P\{^{1}H\}$ NMR spectra of Sn(IV), Pb(II), and Hg(II) complexes of $R_2P(O)$-CS_2^- ligands (R = Ph, Bn) that are of the order S,O > S,S ∼ S, where the P═O group is free in the singly S-bonded, and S,S-bidentate coordination.[40,41] This bidentate S,O downfield shift is significantly smaller than what is observed for the $[Mo_2O_2(\mu\text{-}S)_2]^{2+}$ core, which shows $\Delta(\delta P)$ downfield shifts of 31, 42.8, and 36.2 ppm at room temperature for Ph, Bn, and $PhCH_2CH_2-$ substituents, respectively.[43] In comparison, the $Mo(CO)_4$(dppe) complex, with bidentate dppe ligand, exhibits a large downfield shift of 68.0 ppm that was concluded specific to a five-membered ring strain and bite angle, as well as the size of the metal center.[69] The observed signal for **3**, and its phenyl and benzyl counterparts, at ambient temperature is an average signal for their coordination isomers. The $\Delta(\delta P)$ shift ranks as Sn(IV), Hg(II), Pb(IV) < Mo(V) in **3** < $Mo(CO)_4$(dppe) in good agreement with that **3** has both a smaller metal center (Mo(V) vs Mo(0)) and phosphorus is not the actual donor atom. Low-temperature $^{31}P\{^{1}H\}$ NMR spectra of the complexes possessing phenyl- or benzyl-substituted ligands in solution exhibited five and four different signals for the P atoms, respectively.[43] Interpretation based on electron density on the P atom is that the signals at ∼90 ppm are from the two S,O-bonded coordination, and the two upfield signals are from S, O-bonded coordination plus *cis* and *trans*-DMF coordination (Figure S20). This assumption is corroborated by a $^{31}P\{^{1}H\}$ NMR spectrum of **3** in DMF-d_7 (Scheme 2 and exp.) which exhibits one downfield and two upfield shifts from the average ∼80 ppm in $CDCl_3$ to 89.8 ppm for the S,O-coordination and 72.5/76.8 ppm for the octahedral coordination with *cis*/*trans*-DMF ligands (Scheme 2). Thus, it was expected that the reactions of **3** may show products with multiple coordination isomers and have up to two open coordination sites on each Mo center.

The $^{31}P\{^{1}H\}$ NMR spectrum of **4b** displays a single sharp signal at 66.6 ppm, consistent with a single coordination isomer present at ambient temperature. The structural, NMR, and IR data agree with an S,O-coordination and an overall octahedral geometry around the Mo centers.

Reactions and Kinetics. *Reactions of 3 and 4b with Episulfides and PPh_3.* A comparison of phenyl and benzyl-substituted ligand properties showed that the more soluble benzyl-substituted phosphorus ligand is a more active catalyst in the desulfurization (SAT) of episulfides.[43] Since the phenethyl group is more electron-donating and more organo-soluble, there is a reason to believe that it is a more active SAT catalyst. Reactions of **3** and **4b** with cyclohexene sulfide (CS) and propylene sulfide (PS), and of **3** with styrene sulfide (SS) were run at an ambient temperature in $CDCl_3$. The reactions produce elemental sulfur and alkenes. The formation of elemental sulfur was confirmed by its melting point. Monitoring of the reaction progress was conducted following the desulfurization in the ^{1}H NMR spectra (Figure 2). Analysis

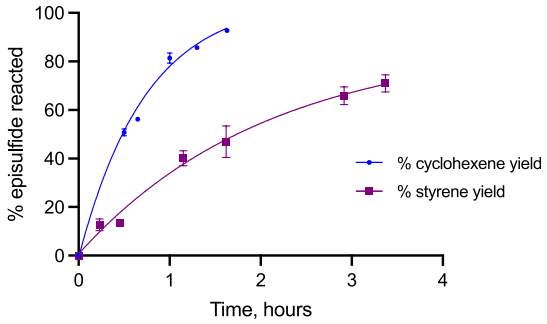

Figure 2. Reaction progress for SAT reactions with **3** (1 mol %) in $CDCl_3$. See text and Table 2 for propylene sulfide data.

determining present products postreaction was performed using ^{1}H and $^{13}C\{^{1}H\}$ NMR data by verifying known chemical shifts. Efforts searching for coordinated alkenes or episulfide by NMR aided by reported cases for $\{CpMo(\mu\text{-}S)_2\}$ dimers,[70] proved fruitless.

Cyclohexene sulfide was about 95% converted to cyclohexene in 2 h while the styrene sulfide reacted more slowly, exhibiting about 70% conversion after 4 h. The catalyst concentrations were varied from 0.1 to 1% mol in reactions of **3** with the episulfides. Selected data for SAT reactions of the episulfides with **3**/**4b** is given in Table 2. Yields were obtained for catalyst loadings higher than 1 mol % in less than 4 h with styrene sulfide and cyclohexene sulfide. Propylene sulfide reaction yields after 4 h were only 24% for 1 mol % of **3**.

Reactions employing **3** as a catalyst for SAT of these episulfides exclusively formed alkenes (Table 2, entries 1−3). The alkene formation is rapid in reactions with cyclohexene sulfide and styrene sulfide, although significantly slower for the latter (Entry 2), and particularly slow with propylene sulfide (Entry 3). The turnover frequency (TOF, Table 2) was calculated to compare the reactions for cyclohexene sulfide and styrene sulfide. TOF for SAT of cyclohexene sulfide desulfurization (221 h^{-1}) is found to be significantly larger than for styrene sulfide (47 h^{-1}) Postreaction mass spectrum evidenced the addition of sulfur to the complex as an intermediate (Figure S32, Table S6).[43] Therefore, a possible mechanism would require sulfur expulsion that could be aided by PPh_3 which is a well-known sulfur abstraction agent. Thus, rhenium catalysts with PPh_3 and episulfides have been reported to give TOF values in the range of 17 to 600 h^{-1} (Table S7)[71,35] and a tungsten complex, with various alkyl and

https://doi.org/10.1021/acs.inorgchem.4c05188
Inorg. Chem. 2025, 64, 4431−4446

Table 2. Selected Reaction Yields for NMR Scale Reactions in $CDCl_3$ of 3 with/without PPh_3, or 4b with Episulfides

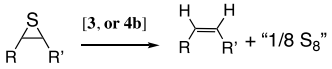

entry	catalyst,	catalyst,[a] mol %	PPh_3,[a] mol %	epi-sulfide	cat./PPh_3, ratio	product (alkene/PTE), %	time, h	conv.%[b]	TOF,[c] h^{-1}
1	3	0.50		CS		100/-	0.47	52	221
2	3	1.0		SS		100/-	0.98	19	47
3	3	1.0		PS		100/-	26.6	42	
4	3	0.50	100	CS	0.0050	100/-	0.42	64	305
5	3	1.0	100	SS	0.010	100/-	0.40	25	80
6	3	0.50	100	PS	0.0050	6.1/93.9	22	93	
7	4b	1.0		CS		100/-	23	26	
8	4b	1.0		PS		100/-	23	7	

[a]w/respect to episulfide. [b]For conversion of episulfide at the time given in the table. [c]mol episulfide reacted/mol catalyst × hour; PS, propylene sulfide; SS, styrene sulfide; CS, cyclohexene sulfide; PTE, polythioether; TOF, mol episulfide reacted per mol complex per hour, or turnover frequency.

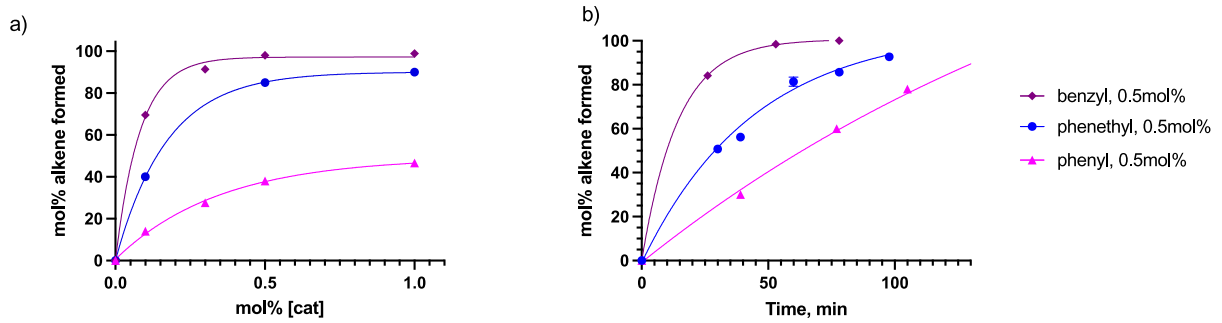

Figure 3. Comparison of reaction yield of cyclohexene for different substituents on the phosphinoyldithioformate ligand (a) reaction yield at 60 min vs concentration of catalyst and, right; (b) function of time for the three catalysts given in the legend. Figure legend: benzyl; $[\{(Bn)_2P(O)CS_2\}_2Mo_2O_2(\mu\text{-}S)_2(DMF)_2]$ and phenyl; $[\{(Ph)_2P(O)CS_2\}_2Mo_2O_2(\mu\text{-}S)_2(DMF)_2]$ adapted from ref 43. Available under a CC-BY 4.0 license, 2021, Razinkov, Ingvarsdottir, Kvaran, Jonsdottir, Suman; phenethyl = 3, this work.

benzyl-substituted dithiolene groups gave TOF values in the range of 5.3 to 17.1 h^{-1} (Table S7).[22]

PPh_3 and the episulfides were used in a ratio of 1:1 based on the hypothesis that the sulfur atom of the episulfides is activated by its interaction with the Mo center (Table 2, entries 4−6). TOF increased for cyclohexene sulfide to 305 h^{-1} and almost doubled for the styrene sulfide to 80 h^{-1}. However, for longer reaction times than 1 h, PPh_3 was found to have a negative impact on the SAT of styrene sulfide, and mainly polythioether was formed in the reactions with propylene sulfide. It was established that **3** is not involved in polythioether formation. In SAT reactions of propylene sulfide with $\{MeReO(edt)\}_2$, (edt = 1,2-ethanedithiolate) and PAr_3 (Ar = aryl), PAr_3 has been reported as a noninnocent reagent coordinating to the dimeric Re complex, forming a less catalytically active mononuclear complex.[26]

Entries 7 and 8 in Table 2 show results for SAT of cyclohexene sulfide and propylene sulfide with **4b**. Both yielded alkenes as products, but the reaction yield was very low within 23 h. In **4a**/**b** the isothiocyanato ligands are positioned *cis* to the Mo═O group (Figure 1). The hypothesis was that they would impact the nonrigid behavior of the ligand O-donors who are positioned *trans* to the molybdenyl group where the bulky ligands folded under the $[Mo_2O_2(\mu\text{-}S)_2]^{2+}$ core (Figure 1) result in less accessibility to the Mo centers leading to diminished reactivity. The experimental data support this hypothesis, where **4b** proved to be sluggish, producing only 26% cyclohexene from cyclohexene sulfide after 23 h.

Figure 3 shows comparative plots of reaction yields for **3**, and for corresponding complexes with phenyl and benzyl substituents[43] for SAT reactions of cyclohexene sulfide as a function of catalyst loading (a), and time (b). Figure 3b shows the conversion of cyclohexene sulfide for the complexes employing 0.5 mol % of the complexes. Interestingly, **3** did not perform better than its counterpart with the benzyl-substituted ligand. The catalytic activity is arranged by substituents as benzyl > phenethyl > phenyl for desulfurization of cyclohexene sulfide. The increased organosolubility of **3** might be expected to improve the catalytic activity since the solubility is an important factor where polar coordinating solvents slow the SAT reaction. However, since the crystal structures revealed that the organic substituents on the phosphinoyl ligands pack *trans* to the molybdenyl groups in solution, they may disperse sufficiently to crowd the substrate access to the molybdenum centers despite dissociation of the dative P═O bond. Furthermore, considering that the benzyl group is less bulky than the phenethyl group and more soluble than the phenyl-substituted complex we conclude that the steric bulk effect competes with the solubility effect in determining the catalytic abilities. Conversely, the substituents on the P atom in **3** reduce the rigidity of the catalysts with an increase in σ-donating abilities. This suggests that the phenyl-substituted complex could become more active if its solubility was improved. Thus, SAT reactions with PAr_3 (Ar- *para*-substituted aryl), propylene sulfide, and $\{MeReO(edt)\}_2$ have been found to yield the slowest reactions with the weakest Lewis base.[26]

https://doi.org/10.1021/acs.inorgchem.4c05188
Inorg. Chem. 2025, 64, 4431−4446

Reactions of **3** with cyclohexene sulfide and with PPh_3 were monitored both by ^1H NMR and $^{31}P\{^1H\}$ NMR to elucidate (a) the sulfur rich intermediate in the reaction of **3** and cyclohexene sulfide, and (b) the specific reaction behavior of PPh_3.

The reaction of propylene sulfide and **3** did not produce the alkene in a significant yield and styrene sulfide product yields were limited in the presence of PPh_3 (Table 2). Although the cyclohexene sulfide initial reaction rate was influenced by the addition of PPh_3, the final reaction yields were similar (Figure 4). The reaction clearly progresses much faster with **3** than the spontaneous reaction of cyclohexene sulfide and PPh_3. The stoichiometric reaction of cyclohexene sulfide with PPh_3 to form cyclohexene is discussed next but it was found to contribute up to about 6% of the final reaction yield (Figure 4).

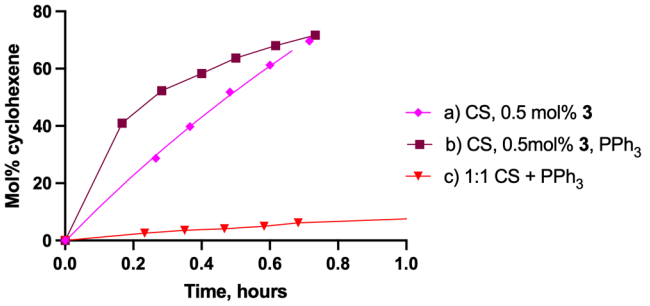

Figure 4. Cyclohexene reaction yields with 0.5 mol % **3**, (a) without and (b) with PPh_3, and (c) contribution from the spontaneous reaction of cyclohexene sulfide (CS) and PPh_3.

SAT of cyclohexene sulfide and **3** in the presence of PPh_3 was monitored with $^{31}P\{^1H\}$ NMR and the disappearance of PPh_3 was quantified. The formation of Ph_3PS and unreacted cyclohexene sulfide is shown in Figure 5 as determined from ^1H NMR spectra. An identified intermediate most likely involves a triply sulfur-bridged complex of **3**, which requires neither a change in the oxidation states of the metal nor a change in the charge of the complex. Triply sulfur-bridged complexes of tungsten and molybdenum are known examples of such complexes.[22,72,73] Two reaction steps are proposed where the initial step is the sulfur addition onto **3**, releasing alkene, and the second step is sulfur expulsion from the complex. The sulfur expulsion reaction is expected to be the rate-limiting step in this reaction based on the steric effects of the sulfur-rich intermediate and the potential bond-breaking energy required for the expulsion. Once PPh_3 is added, the formation of Ph_3PS is comparable to the disappearance of cyclohexene sulfide (Figure 5) suggesting that the alkene formation has now become rate-limiting.

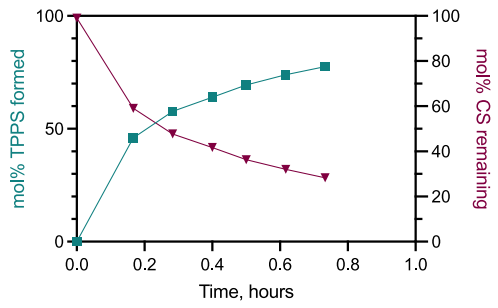

Figure 5. Formation of Ph_3PS in relation to the disappearance of cyclohexene sulfide (CS) over time; 1 mol % **3** with cyclohexene sulfide in the presence of PPh_3 in $CDCl_3$ (CS:PPh_3 is 1:1). TPPS, triphenylphosphine sulfide.

An intermediate with a coordinated PPh_3 was identified by mass spectrometry and the $^{31}P\{^1H\}$ NMR spectrum as a product in the reaction of **3** and PPh_3 (Table S6). This was unexpected, since PPh_3 is often employed as an atom abstraction reagent for OAT or SAT reactions with Mo in oxidation states of +IV or higher,[38,74] and generally favors coordination to organometallic Mo centers with lower oxidation states.[75−77] Careful analysis revealed that the amount of PPh_3S formed was larger than expected. Concerns regarding the PPh_3 reaction behavior led to investigations of both its reactions with the episulfides and with **3**.

Coupling of coordinated PPh_3-P-ligand signals in the $^{31}P\{^1H\}$ NMR may be expected over three to four bonds as shown in Scheme 3 to yield doublets from different coordination modes, while the two P atoms in **3** are sufficiently far apart to negate consideration of potential coupling between them. Experiments confirmed that ligand **2**, does not react with PPh_3 in DMSO-d_6 over 21 h. One to four equivalents of PPh_3 were added to a solution of **3** in $CDCl_3$ and NMR spectra were recorded. Up to 3 equiv showed multiple doublets and weak signals that cleared up at four equiv completely (Figure 6). Thus, integration revealed that 2 equiv coordinated to give five doublets and two singlets (Figure 6B). Surprisingly, a singlet that integrated to ∼0.5 equiv appeared to be from Ph_3PS,[68] as confirmed by $^{13}C\{^1H\}$ NMR spectrum and by verifying its $^nJ(^{31}P-^{13}C)$ coupling constants on an original Ph_3PS sample (experimental section and ref 68. Although the reaction of PPh_3 with disulfide ligand on molybdenum or tungsten complexes to form a terminal sulfido (S^{2-}) group and Ph_3PS is well documented,[61,62,74,78−82] abstraction of a bridging sulfur atom forming Ph_3PS is better known for triple or more sulfur-rich bridges.[22]

Complex **3** exhibits its P signals downfield from the free ligand **2** signal and the new doublets were assigned to P signals of **3**, while the upfield signals were assigned to coordinated PPh_3 (Figure 6). The two PPh_3 signals correspond to the *cis*

Scheme 3. Possible Coordination Modes of PPh_3 and Phosphinoyldithioformate Ligand[a]

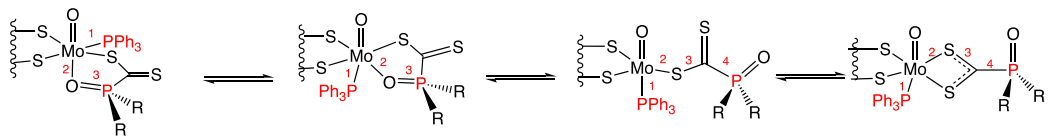

[a]I–IV show different possibilities for $^{31}P-^{31}P$ coupling over **3** or **4** bonds.

https://doi.org/10.1021/acs.inorgchem.4c05188
Inorg. Chem. 2025, 64, 4431−4446

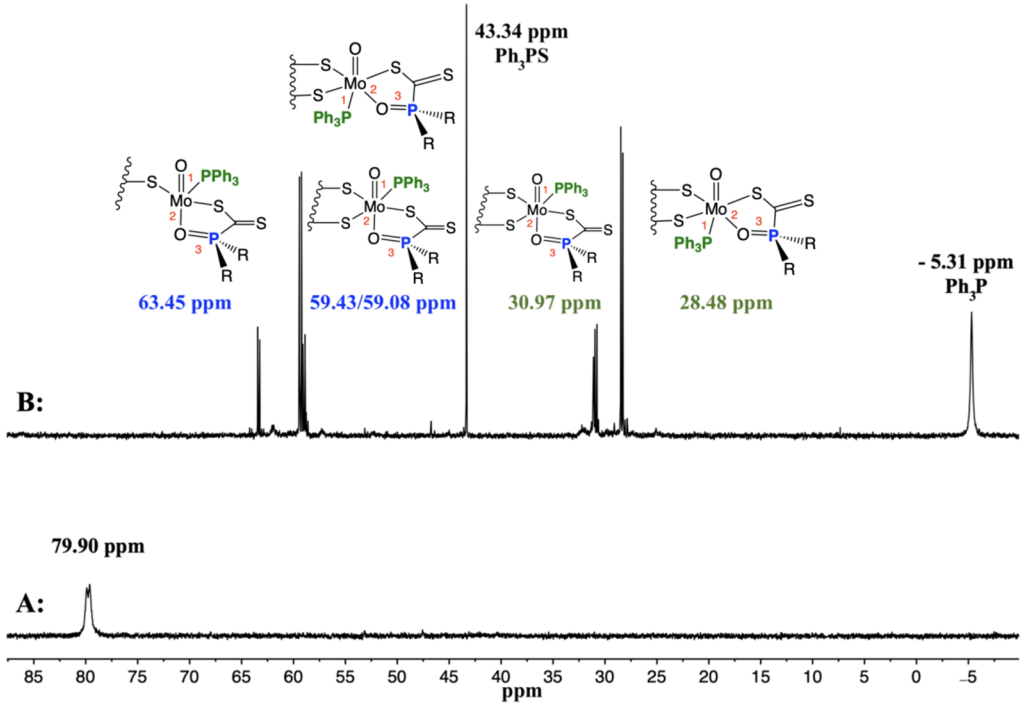

Figure 6. ^{31}P-{^{1}H} NMR spectra of reaction of **3** with PPh_3 (1:4) in $CDCl_3$; (a) before the reaction; (b) postreaction.

and *trans* conformations with respect to the Mo═O group, and they couple with the two signals (I and II in Scheme 3). A broad singlet at 31.10 ppm, which may be a Ph_3PO or $^4J(PPh_3$-$PPh_3)$ signal,[68] was left unassigned.

Three doublets for **3** (Figure 6) are in the vicinity of the sharp singlet signal observed for **4a**/**b**. By analogy, the isothiocyanato and PPh_3 coordinated complexes are expected to have similar coordination geometry in solution. An IR spectrum of a $CHCl_3$ solution for **4b** was obtained to investigate its solution coordination. The spectrum supports that the coordination geometry is S,O- as in the KBr pellet for **4b** and the respective upfield shift of the [**3**-PPh_3] species may be explained by PPh_3 π-acceptor ability compared to that of the nitrogen of the isothiocyanato ligand. Although three equivalents may be sufficient, the addition of the fourth equivalent exhibited fewer sharp signals (Figure S33). While integrations do not give a precise match for the Ph_3PS and the complex signals, a complex with a single bridging sulfur may be observed as the farthest downfield signal (63.45 ppm) possessing the strongest ligand dative O bond to the Mo center.

Polythioether formation in SAT from an episulfide into trivalent phosphorus compounds has not been reported in catalytic studies. Sulfur atom transfer from propylene sulfide to PPh_3 employing catalytic amounts of tungsten complexes,[22] or rhenium complexes,[71] in $CDCl_3$, leads to Ph_3PS and propylene formation. Direct SAT of episulfides into trivalent phosphorus compounds, such as PPh_3, is well-known, but it is reported to be slow and lead to Ph_3PS and alkene formation.[35,83] Direct reaction of PPh_3 and propylene sulfide was found to result in 7% conversion to Ph_3PS in $CDCl_3$ after 24 h.[71] Treatment of propylene sulfide with PPh_3 has given no direct reaction until a catalytic amount of rhenium complex is added.[35] Sulfur atom transfer from propylene sulfide or styrene sulfide to *tri*-anisylphosphine using dithiophosphate molybdenum complex in C_6D_6 leads to the formation of *tri*-anisylphosphine sulfide.[19]

Table 3 shows results for reactions of the episulfides with PPh_3. The products formed depended on the episulfide and on the amount of PPh_3 employed.

Table 3. Selected Reaction Yields and Products for Reactions of PPh_3 with Episulfides

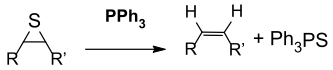

entry	episulfide		RS:PPh_3, ratio	product ratio (alkene/PTE), %	time, h	conversion of episulfide, %
1	CS	**PPh_3**[a]	1.0:1.0	100/-	21	50
2	CS	**PPh_3**[b]	1.0:1.0	100/-	37.4	50
3	SS	**PPh_3**[a]	10:4.0	39/61	20	88
4	SS	**PPh_3**[b]	10:2.0	20/80	1.2	94
5	PS	**PPh_3**[a]	10:1.0	0.5/99.5	1.5	50
6	PS	**PPh_3**[b]	10:0.1	-/100	1.3	100

[a]$CDCl_3$. [b]DMSO-d_6; PTE, polythioether; PS, propylene sulfide; SS, styrene sulfide; CS, cyclohexene sulfide.

Reactions with cyclohexene sulfide were found to be slow (Table 3), in agreement with earlier observations, yielding only the alkene both in $CDCl_3$ and DMSO-d_6.[35,83] However, reactions of PPh_3 with either styrene sulfide (in $CDCl_3$) or propylene sulfide (in DMSO-d_6) form polystyrene- or polypropylene-thioethers, respectively, as the major products. Attempts to increase the alkene yields by lowering the ratio of PPh_3 to episulfide were unsuccessful for both styrene sulfide and propylene sulfide.

Reducing the ratio of PPh_3 to episulfide from 1:1 to 4:6 in a reaction with SS (in $CDCl_3$) formed styrene and polystyrene sulfide (Table 3); Further lowering of the ratio (1.0−10 mol %) resulted in a spontaneous reaction with styrene sulfide to give styrene and unreacted episulfide but no polymers. A

https://doi.org/10.1021/acs.inorgchem.4c05188
Inorg. Chem. 2025, 64, 4431−4446

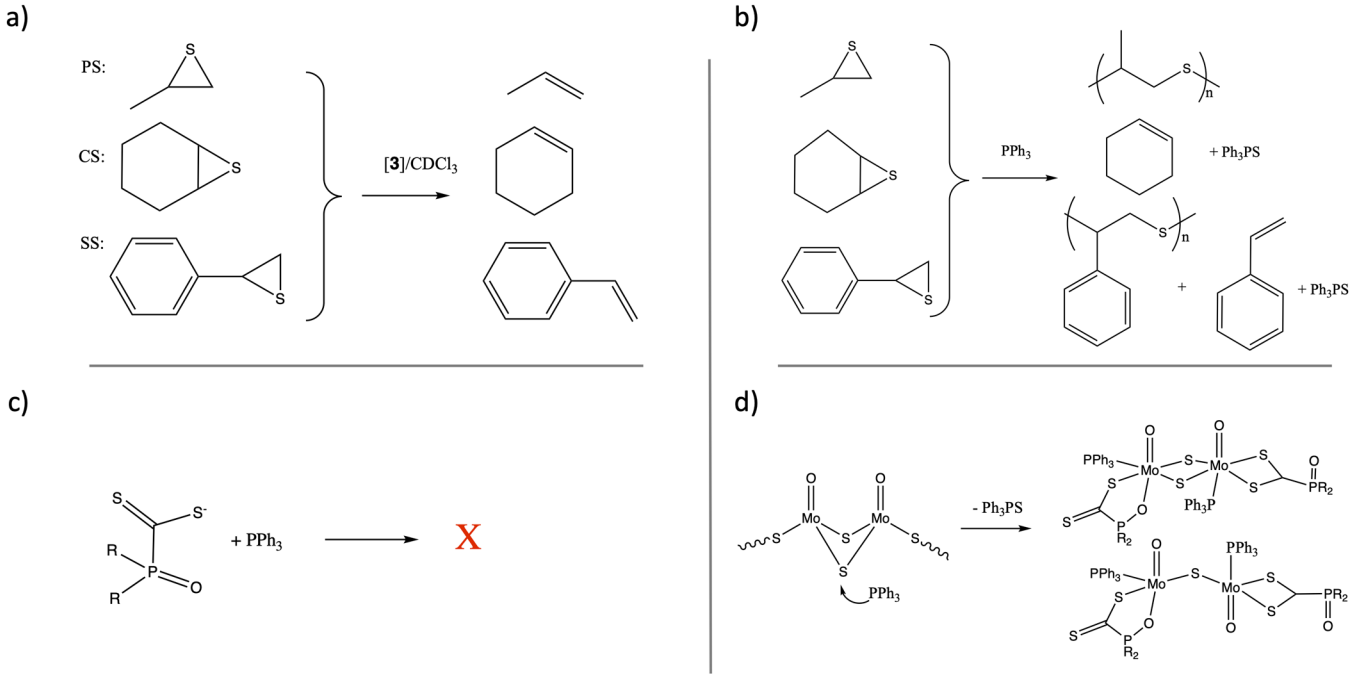

Figure 7. Summary of results obtained from reactions of selected episulfides with (a) complex **3**, (b) with PPh_3, and reactions of PPh_3 with (c) ligand **2**, and (d) complex **3**.

spontaneous reaction with PPh_3 took place until PPh_3 was consumed.

A summary of reactions of **3** with/without PPh_3 is presented in Figure 7. Briefly, the reaction of propylene sulfide with PPh_3 was found to be faster than its reaction with **3**, achieving about 50% reaction yields in 1.5 h (Tables 3 and 2). A stoichiometric reaction of PPh_3 with propylene sulfide resulted in both its polymerization and propylene formation. The reaction of propylene sulfide with a catalytic amount of PPh_3 (10 mol %) in $CDCl_3$ formed polypropylene sulfide and propylene (99.5:0.5% ratio). 50% conversion of propylene sulfide was observed in less than 1.5 h, and 100% conversion was achieved in less than 4 h. Reducing the amount of PPh_3 (0.1 or 0.5 mol %) in $CDCl_3$ formed propylene and unreacted propylene sulfide.

The solvent chosen may play a role since the SAT of cyclohexene sulfide was faster in $CDCl_3$ than in DMSO-d_6 in agreement with other SAT studies showing that coordinating solvents compete with the substrates.[43,84] Reactions with episulfides in DMSO-d_6 appear to favor poly(thioether) formation, although this was not explored in detail.

*Kinetics of Reactions of **3** with Cyclohexene Sulfide and PPh_3.* The $^{31}P\{^1H\}$- and ^1H NMR spectra of **3** in a reaction with excess cyclohexene sulfide were monitored to gain insights into the reaction mechanism (Figure 8).

Before the reaction, coordination isomer signals (S,O-, ±DMF) were grouped together at ∼80 ppm (Figure 8A). Sulfur precipitated during the reaction, and the ^{31}P NMR signal of **3** at ∼80 ppm disappeared completely after the reaction. New sharp signals appeared upfield, and a broad signal appeared downfield. After about 30 min, dissociation of the P═O dative bond to the molybdenum was evidenced by an upfield shift of the methylene proton signals in the ^1H NMR spectrum, and an upfield shift of the ligand signal in the ^{31}P NMR spectrum, close to where the free ligand resides at 43.8 (Table 1), consistent with the change to a single S or/and S,S

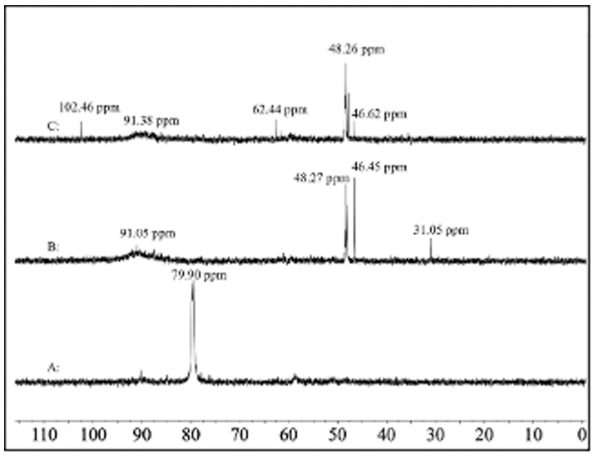

Figure 8. $^{31}P\{^1H\}$ NMR spectra of reaction of **3** with cyclohexene sulfide in $CDCl_3$; (A) before reaction, ^1H NMR shows spectrum of **3** including DMF, (B) during a reaction with cyclohexene sulfide, where ^1H NMR shows spectrum of **3**, cyclohexene sulfide, DMF, and cyclohexene, and (C) postreaction where ^1H NMR shows spectrum of **3**, DMF, cyclohexene. Yellow solid isolated had a mp of 107−110 °C (S_8), $^{13}C\{^1H\}$ NMR shows coordinated ligand, cyclohexene, and DMF.

coordination of the ligand.[40,41] An unknown signal was observed at 31.05 ppm during the reaction of cyclohexene sulfide (Figure 8, part B), which disappeared after the reaction was completed (Figure 8, part C). Assignment of the signals in Figure 8A−C is given in Scheme 4. Considering that the *iso*-bidentate S,S-coordination has a better back bonding ability to the phosphorus atom than the singly S-bonded ligand its signal may be expected to appear downfield from the singly S-bonded isomer signal.[85] The unknown signal, in the vicinity of the Ph_3PO signal position, is not likely to be caused by that, since it is absent at the start and end of the reaction.[68] It could possibly be an effect of intermolecular forces during the SAT

https://doi.org/10.1021/acs.inorgchem.4c05188
Inorg. Chem. 2025, 64, 4431−4446

Scheme 4. Possible Scenarios for the Mechanism of Desulfurization of Cyclohexene Sulfide with 3

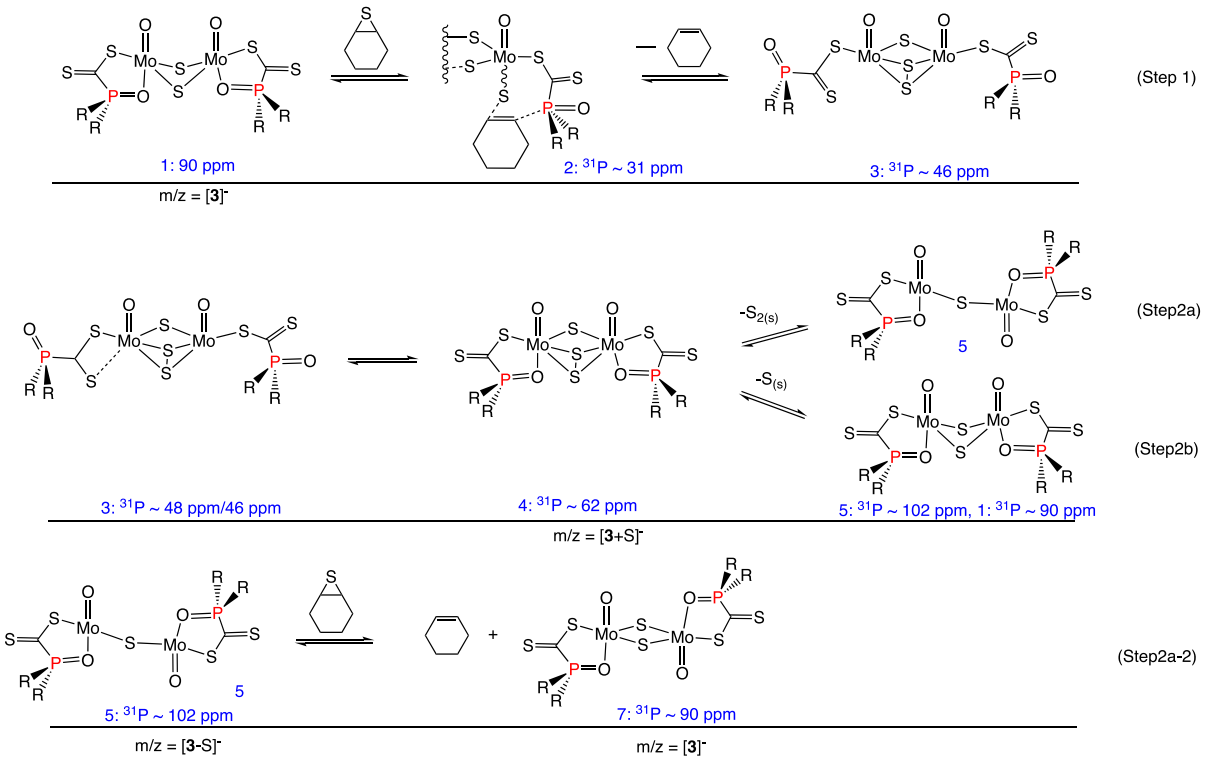

reaction, where the P═O group dissociates and is in sufficient proximity to the cyclohexene sulfide to assist with the reaction. After the reaction was completed, a mixture of the S-, S,S- (48−46 ppm) and S,O-bonded isomers (90−102 ppm) are present (Figure 8C) judging from the signals. Complex **3** survived the reaction judging from mass spectrometry data that show signals for **3** and "**3** + S" ions in the spectrum (Figures S30−32). The signal at 62.44 ppm was assigned to the "**3** + S" isomer in agreement with the $^{31}P\{^{1}H\}$ NMR signal of the isothiocyanato complex which was found at 66.6 ppm (Table 1). Sulfur expulsion may expel one or two sulfur atoms.[34] The signal at 102 ppm is further downfield than the confirmed S/O coordination signal and fits well for a compound with a single sulfur bridge. Expulsion of "S_2" to form singly bridged species and reform doubly bridged **3** during the reaction agrees with the reported accessibility of an *anti*-isomer of the $[Mo_2O_2(\mu\text{-}S)_2]^{2+}$ core requiring bond breaking.[86−88] It follows that the broad signal at 90 ppm was assigned to a mixture of *syn* and *anti* isomers with *cis*/*trans* dative P═O coordination or 6 stereoisomers.

Given that the reactions of **3** with cyclohexene sulfide and styrene sulfide are reasonably paced, its kinetics and potential mechanism were further explored. The following was evident from the experimental data: (a) Ph_3PS was formed in the presence of PPh_3 and **3**, (b) postreaction mass spectrum confirmed that **3** survived and that it added on a sulfur atom, (c) $^{31}P\{^{1}H\}$ NMR shows two unexpected signals, one at 102 ppm, suggesting the presence of a new complex and (d) another signal at 31.05 ppm attributable to intramolecular interaction between the ligand P atom and the alkene, (e) the alkene formed rapidly in a reaction of **3** and PPh_3 exhibiting a saturation curve characteristic for a dissociative mechanism and (f) alkene formed rapidly in a reaction with **3**, apparently in a linear progression, indicative of an associative mechanism (Scheme 4, and Figure 4).

It is proposed that the reaction of **3** and episulfide proceeds in two steps. Scheme 4 gives a possible scenario based on well-known redox abilities of sulfide ligands involving insertion and expulsion of sulfur.[10,11,27,34] The episulfide sulfur adds to one Mo center, and the dative P═O bond dissociates (Scheme 4, (1)). With the help of the P atom on **2,** the sulfur is inserted into a Mo−S bond, leading to the breaking of the Mo−S bond of the second Mo center (2). The alkene is released, and a "S_2" group is expelled (step 2a). With only one sulfur bridge, rotation of the Mo═O groups may take place for some centers to form the *anti* isomer before a second episulfide enters (steps 2a-2) and the two previous steps are repeated. A sulfur-rich bridge with one or two S_2^{2-} ligands may also expel elemental sulfur and exist in the *syn* orientation (step 2b). Species labeled 2 and 3 were observed in the reaction of **3** and cyclohexene sulfide (Scheme 4). The release of the alkene and the sulfur expulsion are two separate steps where the alkene is released directly but the sulfur expulsion is likely to be sterically controlled. Sulfur-rich bridges usually entail four sulfur atoms, although here multiple sulfur atoms (>3) were not evidenced.[89,90]

With added PPh_3, coordination to the Mo center takes place as shown in Scheme 3, and PPh_3 can attack the bridging sulfur as soon as the episulfide coordinates in step 1 (Scheme 3). Ph_3PS is formed as fast as the episulfide can coordinate to Mo or enter its vicinity, possibly nonspecifically toward a bridging sulfur vs episulfide sulfur. In Figure 4 a, saturation curve is observed for the SAT reaction in the presence of PPh_3 as is typical for a dissociative mechanism, in this case, the sulfur abstraction reaction. The PPh_3 coordination causes steric crowding which likely explains the slowing down of the reaction between **3** and styrene sulfide in its presence. Because

https://doi.org/10.1021/acs.inorgchem.4c05188
Inorg. Chem. 2025, 64, 4431−4446

of these observations and the identification of intermediates, we propose that the mechanism changes from an additive to a dissociative rate-determining step upon the addition of PPh_3. The microscopic mechanism is complicated, however. Much lower activity of **4b** is explained by the presence of its isothiocyanato ligands limiting access to the Mo center and the ligand P atom to form "**3**-S" in Scheme 5.

Scheme 5. Proposed Main Steps in Reactions of 3 with Episulfides (ES) (a) without PPh_3 and (b) with PPh_3

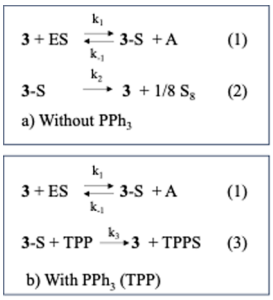

Rate of Reactions of CS and SS with ***3***. The mechanism for alkene (E) formation is associative in nature and second-order dependent on both the **3** and episulfide concentrations. The sulfur expulsion reaction shown in Scheme 5a (2) is assumed to be dissociative, while the sulfur abstraction reaction with PPh_3 is associative. The consequences of the changes in the rate-determining step (a) without and (b) with PPh_3, are apparent from the linear alkene formation (a) to a saturation curve (b) shown in Figure 4. Step 1 is shared in both cases (a) and (b) in Scheme 5. Different episulfides (ES) were expected to react at different rates, while the sulfur expulsion reaction is assumed independent of the organic compound properties.

The kinetics for the reactions of concern for ES = CS and SS were evaluated to explore the hypothesis of the potential reversibility of the SAT reaction. The different results obtained for the episulfides evoked questions regarding the reaction mechanism, i.e., whether all three (CS, SS, and PS) proceed through the same mechanism for the desulfuration reaction. The cyclohexene sulfide is the most activated episulfide, while styrene sulfide, which is bulkier and has two enantiomers, is less activated. The propylene sulfide conversion to propylene was surprisingly slow, considering its small size and activated sulfur atom despite having two enantiomers. Data sets for the reaction of **3** with two episulfides (CS and SS) were chosen for further study of the reaction mechanism and rates for the formation of the alkene.

Data of the episulfide (ES) and the corresponding alkene (A) concentrations as a function of time for the two reactions were compared to a kinetic model derived for the simplified reaction, Scheme 5a (SI Appendix 1). The following assumptions were made: first, steady-state conditions to the sulfurated complex (**3**-S), during the reactions, were assumed (i.e., $d[\mathbf{3}\text{-S}]/dt = 0$), second, the concentration of the free complex was assumed to be a lot larger than the sulfurated form (i.e., $[\mathbf{3}] \gg [\mathbf{3}\text{-S}]$) and third, the rate of sulfur removal from **3**-S by the direct expulsion (Scheme 5, reaction 2) was assumed to be faster than by the reverted reaction 1 (i.e., $k_2 \gg k_{-1}[A]$). This allowed a derivation of the expression,

$$\frac{v(A)}{[\mathbf{3}]_0[ES]} = k_1 - \{\frac{k_{-1}k_1}{k_2}\}[A] \quad (1)$$

where $v(A)$ is the rate of formation of alkene, A (i.e., $v(A) = d[A]/dt$). Equation 1 corresponds to a linear relationship between $v(R)/([\mathbf{3}]_0[ES])$ and [A] which should allow evaluation of k_1 and the ratio k_{-1}/k_2 from the intersect and slope values of a line fit. $v(A)$ (= $d[A]/dt$) was determined from the concentration of A ([A]) as a function of time (t) after fitting the data point by a functional form corresponding to a pseudo-first-order formation reaction for A. Figure 9

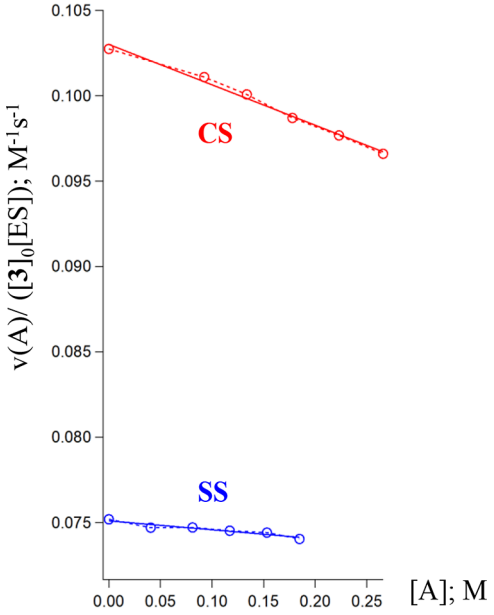

Figure 9. $v(R)/([\mathbf{3}]_0[ES])$ vs [A] for ES = CS ($[\mathbf{3}]_0$ = 0.00114 M, $[CS]_0$ = 1.134 M; top, red) and SS ($[\mathbf{3}]_0$ = 0.00112 M, $[SS]_0$ = 1.122 M; bottom, blue). See main text.

shows results of the kinetic model for two sets of data points for RS = CS and SS. The linear behavior of $v(A)/([\mathbf{3}]_0[ES])$ vs [A] observed strongly suggests that the kinetic model (Scheme 5a and the above-mentioned assumptions) applies for the two reactions of concern. Slope and intersect values of linear fit functions differ significantly for the two reagents. Analyses based on eq 1 result in evaluations of the rate constants k_1 = 0.103 M^{-1} s^{-1} and k_1 = 0.075 M^{-1} s^{-1} for CS and SS, respectively (i.e., $k_1(CS) \geq k_1(SS)$) as well as k_{-1}/k_2 of about k_{-1}/k_2 = 0.23 M^{-1} for CS and k_{-1}/k_2 = 0.07 M^{-1} for SS (i.e., $k_{-1}/k_2(CS) > k_{-1}/k_2(SS)$). Since k_2 is independent of ES, the latter results correspond to $k_{-1}(CS) > k_{-1}(SS)$.

Thus, the analyses give rate constants for the alkene formation of the same order of magnitude for CS and SS, although, as expected, the cyclohexene sulfide was a bit faster compared to the styrene sulfide. It is possible that this first step in the metal-mediated reaction is reversible, at least for some substrates. First and second-order rate constants reported for SAT with rhenium catalysts were reported as 0.98 s^{-1} and 0.25 to 5.58 M^{-1} s^{-1} (SI Table S7).[25,26] SAT reactions with $AsPh_3$ are reported faster than their PPh_3 counterparts because of their lower Lewis basicity.[25,26] In this respect, the rate constants obtained here without PPh_3 are within the range of reported SAT data.

Rate of Reaction of Cyclohexene Sulfide with ***3*** *in the Presence of* PPh_3. Data of CS and the corresponding alkene (C) concentrations as well as for PPh_3 (TPP) and its sulfide (TPPS) as a function of time was compared to a kinetic model

https://doi.org/10.1021/acs.inorgchem.4c05188
Inorg. Chem. 2025, 64, 4431−4446

derived for the simplified reaction Scheme 5b (SI Appendix 2). Steady-state conditions with respect to the sulfurated complex (**3**-S), during the reactions, were assumed (i.e., d[**3**-S]/dt = 0) and the concentration of the free complex was assumed to be a lot larger than the sulfurated form (i.e., [**3**] ≫[**3**-S]). This allowed a derivation of the expression,

$$\frac{[3]_0[ES]}{\nu(TPPS)} = \{\frac{k_{-1}}{k_3k_1}\}\frac{[A]}{[TPP]} + \{\frac{1}{k_1}\} \quad (2)$$

where ν(TPPS) is the rate of formation of triphenylphosphine sulfide (i.e., ν(TPPS) = d[TPPS]/dt). Equation 2 corresponds to a linear relationship between ([**3**]$_0$[ES])/ν(TPPS) and [A]/[TPP], which should allow evaluation of k_1 and the ratio k_{-1}/k_3 from the intersect and slope values. v(TPPS) (= d[TPPS]/dt) was determined from the concentration of triphenylphosphine sulfide ([TPPS]) as a function of time (t) after fitting the data point by a functional form corresponding to a pseudo first-order formation reaction for TPPS. In short, the nonlinear plot of ([**3**]$_0$[ES])/ν(TPPS) vs [A]/[TPP] was obtained, suggesting that simplified Scheme 5b is not satisfactory enough and that more/other reactions need to be considered. The observed coordination of PPh_3 to a sulfur-deficient Mo center further confirms this conclusion (Figure 6).

CONCLUSIONS

The reactivity of **3** was explored with three episulfides: cyclohexene sulfide (CS), styrene sulfide (SS), and propylene sulfide (PS), all of which produced the corresponding alkenes. The addition of PPh_3 with the intention of improving a proposed sulfur expulsion second step in the SAT reaction led to unexpected results which inspired additional studies of the reaction of PPh_3 with both the episulfides and **3** that were conducted. Monitoring of the reactions with $^{31}P\{^1H\}$ NMR proved informative, revealing coordination isomers of **3** with PPh_3. Dissolution results in dissociation of the DMF ligands and dissociation of the dative P═O bond. The isothiocyanate coordinated complex **4** is stable in solution, and its characterization was invaluable in identifying the coordination isomers of **3** by $^{31}P\{^1H\}$ NMR. S,O-coordinated species of **3** with DMF, PPh_3, and S were assigned based on the ^{31}P chemical shifts observed. The upfield shifts of **3** with these added coordinated ligands were ordered as PPh_3 > S^{2-} > SCN^- > DMF assuming the bond strength of the dative Mo−O bond to be weaker with a stronger donor ligand. A possible mechanism was postulated based on the $^{31}P\{^1H\}$ NMR and mass spectrometry data (Figure 8, Scheme 4). The formation of an *anti* coordination isomer of **3** was evidenced in the NMR data, strongly supporting bond breaking and reforming of the sulfur bridges. Bond breaking of the bridging sulfur atoms explains the formation of Ph_3PS in a reaction of **3** and PPh_3, although another reported example of these bridges breaking in the $[Mo_2O_2(\mu\text{-}S)_2]^{2+}$ core requires heating. Coordination of the PPh_3 is better known for coordination to a low valent Mo organometallic center and was quite unexpected. In these aspects, **3** behaves like an electron-rich metal center despite its formal oxidation state of +V.

Observing a slow down of the SAT reaction of SS in the presence of PPh_3 led to the exploration of stoichiometric reactions of the episulfides and PPh_3 that led to different product distribution depending on the episulfide that also depended on the ratio of PPh_3 employed for PS and SS. When **3** and PPh_3 were employed together, CS and SS produced the alkenes at increased reaction rates, while PS formed mostly polythioether. Although the polythioether is formed in stoichiometric reactions with PPh_3, lowering its ratio significantly may avoid polythioether formation.

Comparison of **3** with the complex possessing the analogous benzyl-substituted ligands revealed less reactivity despite increased solubility, as may be expected from the crystal structure, which shows organic substituents to be bulky and to reside below the plane of the $[Mo_2O_2(\mu\text{-}S)_2]^{2+}$ core. Although the P═O dative bond dissociates in a solution, the bulky ligands may disperse around the core for the SAT reaction in nonpolar solvents. It is also unlikely that **3** participates in polythioether formation. **4b** was found to be rather unreactive as was expected for isothiocyanato ligands to render a rigid octahedral coordination geometry around the Mo centers.

In this study, propylene sulfide yielded significantly less alkene than expected for its small size leading to speculation regarding reversibility of the SAT. Attempts to kinetically evaluate its reversibility concluded that it may be reversible for some substrates. Kinetic analysis concluded that the sulfur expulsion step in the presence of PPh_3 is not straightforward and undefined reactions influence the reaction kinetics, which supports that bond breaking and intermolecular interactions may play a role.

EXPERIMENTAL SECTION

General Consideration. Infrared spectra were obtained with a Smart Omni-Transmission Nicolet iS10 spectrophotometer in the range of 4000−400 cm^{-1}. NMR spectra were recorded on a Bruker Avance NEO 400 MHz spectrometer operating at 400.1, 100.6, and 162 MHz for ^1H, $^{13}C\text{-}\{^1H\}$, and $^{31}P\text{-}\{^1H\}$, respectively. The deuterated solvents served as a lock in the ^1H, $^{13}C\text{-}\{^1H\}$ and $^{31}P\text{-}\{^1H\}$ measurements. The parameter used references 85% H_3PO_4 as an external standard. UV−visible spectra were recorded on Agilent Cary 3500 Multicell P UV−vis spectrophotometer. Mass spectra were recorded on a Bruker Compact micrOTOF-Q spectrometer, equipped with an E-spray atmospheric pressure ionization chamber (ESI). Formiat standard was used for calibration both in positive and negative mode. The melting point of isolated sulfur samples was recorded on BUCHI Melting Point M-560 from 50 to 140 °C at a temperature rate increase of 5 °C/min. Elemental analyses were obtained from Midwest Microlab, IN, United States.

Reagents and solvents were purchased from Sigma-Aldrich and used without further purification unless otherwise stated. Deuterated solvents were used as obtained from Sigma-Aldrich. $(Me_4N)_2[Mo_2O_2(\mu\text{-}S_2)(Cl)_4]$,[45] $\{(Ph)_2P(O)CS_2\}_2Mo_2O_2(\mu\text{-}S)_2(DMF)_2$, $\{(Bn)_2P(O)CS_2\}_2Mo_2O_2(\mu\text{-}S)_2(DMF)_2$,[43,91] and $(Et_4N)SCN$ and $(Bu_4N)SCN$,[92,93] were prepared by published methods.

Syntheses. *$(Et_4N)SCN$.* $Et_4NCl{\cdot}H_2O$ (3.68 g, 20 mmol) was added to a solution of KSCN (2.0 g, 20 mmol) in absolute ethanol (100 mL). After stirring for 30 min white precipitate (KCl) was removed by filtration, and the solvent was removed under reduced pressure. The white precipitate was dried in vacuo. Yield: 3.7 g (99%). M.p.: 242 °C. FT-IR (cm^{-1}): ν(SCN), 2056 (vs). ^1H NMR ($CDCl_3$-d_1) δ, ppm: 3.36 (q, 8H, CH_2), 1.32 (tt, 12H, CH_3). $^{13}C\{^1H\}$ NMR ($CDCl_3$-d_1) δ, ppm: 130.83 (s, SCN), 52.66 (t, C−H_3), 7.70 (s, C−H_2).

$(Bu_4N)SCN$. Bu_4NBr (6.47 g, 20 mmol) was prepared in an analogous method as the Et_4N^+ salt. The white precipitate was dried in vacuo. Yield: 5.95 g (99%). M.p.: 119−120 °C. FT-IR (cm^{-1}): ν(SCN), 2055 (vs). ^1H NMR ($CDCl_3$-d_1) δ, ppm: 3.32 (t, 8H, CH_2), 1.67 (t, 8H, CH_2), 1.45 (t, 8H, CH_2), 0.99 (t, 12H, CH_3). $^{13}C\{^1H\}$ NMR ($CDCl_3$-d_1) δ, ppm: 130.96 (s, SCN), 58.89 (s, C−H_3), 24.09 (s, C−H_2), 19.83 (s, C−H_2), 13.75 (s, C−H_2).

*$(PhCH_2CH_2)_2P(O)H$, **1**.* (2-Bromoethyl)benzene (101 mL, 73 mmol) in dry diethyl ether (200 mL) was added dropwise to Mg

https://doi.org/10.1021/acs.inorgchem.4c05188
Inorg. Chem. 2025, 64, 4431−4446

turnings (18.1 g, 73 mol) in dry diethyl ether (150 mL). Dibutyl phosphite (42.5 mL, 21 mol) in diethyl ether (150 mL) was added dropwise to the solution. When all reactants were added, the solution was refluxed for 20 min; 10% HCl solution (370 mL) was slowly added. The water phase was separated from the organic phase. The organic phase was washed with 2% HCl (10 × 150 mL). The water phase was extracted with toluene (5 × 75 mL). The organic phases were combined and dried with Na_2SO_4 overnight, filtered and solvents were removed by rotary evaporation. Diethyl ether (50 mL) was added to the yellow oil and kept at −18 °C overnight. The white crystalline material was filtered off, washed with diethyl ether (50 mL), and dried in vacuo. Yield: 41 g (76%). FT-IR, (cm^{-1}): ν(P(O)H), 2306 (vs), ν(P═O), 1221 (vs), 1160 (s), 1129 (s). ^{1}H NMR ($CDCl_3$-d_1) δ, ppm: 6.90 (d, J = 452 Hz, 1H, P(O)H), δ 7.33, 7.23 (m, 4H, m, 6H, C−H_o, C−H_m, C−H_p), 3.07 (m, C−H_2, 4H), 2.21 (m, C−H_2, 2H), 2.08 (m, C−H_2, 2H). ^{31}P{^{1}H} NMR ($CDCl_3$-d_1) δ, ppm: 30.96 (s). ^{13}C{^{1}H} NMR ($CDCl_3$-d_1) δ, ppm: 140.14, (d,^3J(P−C_i),12.12 Hz), 128.78, 128.17, 126.67 (s, C_o, C_m, C_p), 30.20 (d,^1J(P-CH_2), 63.63 Hz), 27.86 (d,^2J(P-CH_2), 4.04 Hz). UV/vis (DMF, 2 × 10^{-4} M), nm (ε, M^{-1} cm^{-1}): 268 (2898). ESI-MS: [M + Na]$^+$ = $C_{16}H_{19}OPNa^+$ (m/z = 281.1066); found m/z = 281.1063.

K{(PhCH$_2$CH$_2$)$_2$P(O)CS$_2$}(C$_4$H$_8$O$_2$)$_{0.5}$, K[2]. KOH (3.6 g, 57.6 mmol) in water (5 mL) and CS_2 (4.4 g, 57.6 mmol) were added to a solution of bis(phenylethyl)phosphine oxide (15.0 g, 57.6 mmol) in THF (100 mL). The solution changed from colorless to dark red. After stirring for 15 h, water was removed (lower layer). THF was removed under reduced pressure and the dark red oil residue solidified when left in vacuo overnight. 1,4-dioxane (50 mL) was added to the solution and diethyl ether until turbid and placed in a freezer at −18 °C overnight. The dark red microcrystalline solid was filtered off, washed with diethyl ether, and dried in vacuo. Yield: 13.2 g (55%). FT-IR (cm^{-1}): ν(CS_2), 1079 (m), 1036 (vs), 911 (w), (P═O), 1215 (w), 1205 (m), 1153 (s), 1128 (s). ^{1}H NMR (400 MHz, D_2O) δ, ppm: 7.25, 7.15 (m, 4H, m 6H, C−H_o, C−H_m, C−H_p), 3.75 (s, 4H, dioxane), 2.79 (m, 4H, C−H_2), 2.43 (m, 2H, C−H_2), 2.16 (m, 2H, C−H_2). ^{31}P{^{1}H} NMR (162 MHz, D_2O) δ, ppm: 43.6(s). ^{13}C{^{1}H} NMR (101 MHz, D_2O) δ, ppm: 256.58 (d,^1J(P-CS_2), 62.62 Hz), 141.39 (d,^3J(P−C_i), 14.14 Hz), 128.71, 128.20, 126.38 (s, C_o, C_m, C_p), 66.55 (s, dioxane), 29.80 (d,^1J(P-CH_2), 62.62 Hz), 27.39 (d,^2J(P-CH_2), 3.03 Hz). UV/vis (DMF, 7 × 10^{-5} M), nm (ε, M^{-1} cm^{-1}): 362 (11882). UV/vis (DMF, 1.4 × 10^{-4} M), nm (ε, M^{-1} cm^{-1}): 472 (61). ESI-MS: [M^-] = $C_{17}H_{18}OPS_2$ (m/z = 333.0542); found, m/z = 333.0512. Anal. Calc. for $C_{17}H_{18}KOPS_2$ C 54.78, H 5.32. Found: C 55.09, H 5.17.

(Me$_4$N){(PhCH$_2$CH$_2$)$_2$P(O)CS$_2$}, (Me$_4$N)[2]. Me_4NCl (0.303 g, 2.71 mmol) was added to a stirred solution of K{$(PhCH_2CH_2)_2P(O)CS_2$}$(C_4H_8O_2)_{0.5}$ (1.129 g, 2.71 mmol) in CH_2Cl_2 (20 mL). After stirring for 4 h, the solution changed color from dark red to purple, and a white precipitate (KCl) was filtered off, and the solvent was removed under reduced pressure. Dark purple oil was dissolved in 10 mL of DMF, and diethyl ether was added until turbid. The purple solid was filtered off and dried in vacuo. Yield: 0.83 g (75%). FT-IR (cm^{-1}): ν(CS_2), 1029 (vs), 898 (w), ν(P═O), 1210 (m), 1198 (m), 1167 (vs). ^{1}H NMR (400 MHz, D_2O) δ, ppm: 7.32 (m, 4H, m, 6 H, C−H_o, C−H_m, C−H_p), 3.16 (s, 12H, C−H_3), 2.87 (m, 4H, C−H_2), 2.53 (m, 2H, C−H_2), 2.34 (m, 2H, C−H_2). ^{13}C{^{1}H} NMR (D_2O) δ, ppm: 256.69 (d, ^0J(P-CS_2), 62.62 Hz), 141.49 (d,^3J(P−C_i), 14.14 Hz), 128.76, 128.23, 126.43 (s, C_o, C_m, C_p), 55.24 (t, C−H_3), 30.03 (d,^1J(P-CH_2), 63.63 Hz), 27.32 (d,^2J(P-CH_2), 14.14 Hz). ^{31}P{^{1}H} NMR (D_2O) δ, ppm: 43.79 (s). ESI-MS: [M^-] = $C_{17}H_{18}OPS_2$ (m/z = 333.0542); found, m/z = 333.0533. UV/vis (DMF, 6.38 × 10^{-5} M), nm (ε, M^{-1} cm^{-1}): 363 (11776), 473 (65).

{(PhCH$_2$CH$_2$)$_2$P(O)CS$_2$}$_2$Mo$_2$O$_2$(μ-S)$_2$(C$_3$H$_7$NO)$_2$, 3. $(Me_4N)_2[Mo_2O_2(\mu\text{-}S)_2(Cl)_4]$ (0.17 g, 0.30 mmol) were dissolved in DMF (7 mL). (Me$_4$N){$(PhCH_2CH_2)_2P(O)CS_2$} (0.25 g, 0.60 mmol) in DMF (5 mL) was added to the solution. After stirring for 1 h, the solution changed color and a white precipitate formed (Me_4NCl). Diethyl ethyl (30 mL) was added to incipient precipitation of Me_4NCl and the precipitate was allowed to settle for 10 min. After filtration, solvents were removed under reduced pressure. Dark red solid was isolated by filtration, washed with diethyl ether (50 mL), and dried in vacuo. Yield: 0.23g (70%). FT-IR (cm^{-1}): ν(C═O), 1641 (s), ν(P═O), 1214 (w), 1179 (w), 1071 (vs); ν(CS_2), 1053 (vs), 862 (w), ν(Mo═O), 943 (s), ν(Mo−S_b), 476. ^{1}H NMR (400 MHz, $CDCl_3$-d_1) δ, ppm: 8.03 (s, 1H, C(O)H), 7.33 (m, 17H, C−H), 7.01 (m, 3H, C−H), 3.48 (m, 2H, CH_2), 3.19 (m, 2H, CH_2), 2.96 (s, 3H, CH_3), 2.87 (s, 3H, CH_3), 2.78 (m, 8H, CH_2), 2.46 (m, 4H, CH_2). ^{31}P{^{1}H} NMR ($CDCl_3$-d_1) δ, ppm: 80.05, 79.74. ^{31}P{^{1}H} NMR (DMF-d_7) δ, ppm: 89.78, 76.80, 72.51. ^{13}C{^{1}H} NMR ($CDCl_3$-d_1) δ, ppm: 241.66, (d,^1J(P-CS_2) 51.51 Hz), 163.62 (s, C(O)H), 139.37, 138.94 (d, d,^3J(P−Ci), 14.14, 15.15 Hz), 128.90, 128.82, 128.23, 128.16, 127.01, 126.95 (s, C_o, C_m, C_p), 36.98 (s, C−H_3), 31.92 (s, C−H_3), 30.10, 29.85 (dd,^1J(P-CH_2), 61.61, 64.64 Hz), 27.12, 27.08 (dd,^2J(P-CH_2), 18.18, 18.18 Hz). UV/vis (DMF, 1.22 × 10^{-5} M), nm (ε, M^{-1} cm^{-1}): 290 (sh), 359 (18770), 456 (2008). ESI-MS: [M + $C_2H_5O^-$-2C_3H_7NO]$^-$ = $C_{36}H_{41}Mo_2O_5P_2S_6$ (m/z = 1001.8877); found m/z = 1002.0222. Elemental Anal. Calc. for $C_{40}H_{50}Mo_2N_2O_6P_2S_6$: C, 43.63; H, 4.58; N, 2.54. Found: C, 43.57; H, 4.60; N, 2.11%.

(Et$_4$N)$_2$[{(PhCH$_2$CH$_2$)$_2$P(O)CS$_2$}$_2$Mo$_2$O$_2$(μ-S)$_2$(SCN)$_2$], 4a. (Et_4N)SCN (0.10 g, 0.53 mmol) was added to a stirred solution of **3** (0.291 g, 0.265 mmol) in DMF (10 mL). After stirring for 30 min, DMF was removed under reduced pressure. An orange solid was isolated by filtration, washed with ethanol (20 mL) and diethyl ether (50 mL), and dried in vacuo. Yield: 0.28 g (80%). FT-IR (cm^{-1}): ν(SCN), 2086 (vs), ν(P═O), 1217 (w), 1182 (w), 1171 (m), 1096 (s); ν(CS_2), 1052 (vs), 831 (w), ν(Mo═O), 935 (s), ν(Mo−S_b), 482. ^{1}H NMR (CD_3CN-d_3) δ, ppm: 7.34 (m, 9H, C−H), 7.12 (m, 8H, C−H), 6.65 (m, 3H, C−H), 3.16 (q, J = 7.26 Hz, 16H, CH_2), 2.77 (m, 4H, CH_2), 2.60 (m, 2H, CH_2), 2.36 (m, 4H, CH_2), 2.23 (m, 2H, CH_2), 2.03 (m, 2H, CH_2), 1.82 (m, 2H, CH_2), 1.20 (tt, 24H, CH_3). ^{31}P{^{1}H} NMR ($(CD_3)_2CO$-d_6) δ, ppm: 65.91 (s). ^{13}C{^{1}H} NMR (DMSO-d_6) δ, ppm: 242.45 (d,^1J(P-CS_2) 59.59 Hz), 142.83 (s, SCN), 141.69, 140.97 (d, d,^3J(P−C_i), 16.16, 17.17 Hz), 128.69, 128.58, 128.40, 128.29, 127.99, 127.66, 126.11, 125.76 (s, C_o, C_m, C_p), 51.41 (t, C−H_3), 30.69, 27.76 (d, d^1J(P-CH_2), 60.6, 67.67 Hz), 26.06 (d,^2J(P-CH_2), 19.19 Hz), 7.09 (s, C−H_2). UV/vis (DMF, 1.296 × 10^{-5} M), nm (ε, M^{-1} cm^{-1}): 362 (19754), 458 (1826). ESI-MS: [M + $C_2H_5O^-$-2(Et_4NSCN)]$^-$ = $C_{36}H_{41}Mo_2O_5P_2S_6$ (m/z = 1001.8877); found m/z = 1001.8385. Elemental Anal. Calc. for $C_{52}H_{76}Mo_2N_4O_4P_2S_8$: C, 46.9; H, 5.75; N, 4.2. Found: C, 46.39; H, 5.51; N, 4.36%.

(Bu$_4$N)$_2$[{(PhCH$_2$CH$_2$)$_2$P(O)CS$_2$}$_2$Mo$_2$O$_2$(μ-S)$_2$(SCN)$_2$], 4b. (Bu_4N)SCN (0.16 g, 0.53 mmol) was added to a stirred solution of **3** (0.29 g, 0.265 mmol) in DMF (10 mL). After stirring for 30 min, DMF was removed under reduced pressure. An orange solid was isolated by filtration, washed with ethanol (20 mL) and diethyl ether (50 mL), and dried in vacuo. Yield: 0.32 g (78%). FT-IR (cm^{-1}): ν(SCN), 2082 (vs), ν(P═O), 1216 (w), 1099 (s); ν(CS_2), 1052 (vs), 830 (w), ν(Mo═O), 939 (s), ν(Mo−S_b), 480. ($CHCl_3$, cm^{-1}): ν(SCN), 2088 (vs), ν(P═O), 1216 (vw), 1100 (s); ν(CS_2), 1052 (vs), ν(Mo═O), 939 (s), ν(Mo−S_b), 478. ^{1}H NMR ($CDCl_3$-d_1) δ, ppm: 7.33 (m, 3H, C−H), 7.21 (m, 5H, C−H), 7.09 (m, 9H, C−H), 6.68 (m, 3H, C−H), 3.32 (t, 16H, CH_2), 2.74 (m, 6H, CH_2), 2.34 (m, 4H, CH_2), 2.11 (m, 2H, CH_2), 1.96 (m, 2H, CH_2), 1.70 (m, 2H, CH_2), 1.66 (qui, 16H, CH_2), 1.42 (sextet, 16H, CH_2), 0.96 (t, 24H, CH_3). ^{31}P{^{1}H} NMR ($CDCl_3$-d_1) δ, ppm: δ 66.58 (s). ^{13}C{^{1}H} NMR ($CDCl_3$-d_1) δ, ppm: 242.55 (d,^1J(P-CS_2) 56.56 Hz), 143.84 (s, SCN), 141.52, 141.42 (d, d,^3J(P−C_i), 16.16, 16.16 Hz), 129.25, 128.78, 128.51, 128.46, 128.26, 128.16, 126.25, 125.81 (s, C_o, C_m, C_p), 58.72 (s, C−H_3), 31.42, 28.73 (d, d^1J(P-CH_2), 61.61, 68.68 Hz), 27.02 (d,^2J(P-CH_2), 24.24 Hz), 24.12 (s, C−H_2), 19.89 (s, C−H_2), 13.94 (s, C−H_2). UV/vis (DMF, 1.284 × 10^{-5} M), nm (ε, M^{-1} cm^{-1}): 362 (19309), 458 (1926). ESI-MS: [M + $C_2H_5O^-$-2(Bu_4NSCN)]$^-$ = $C_{36}H_{41}Mo_2O_5P_2S_6$ (m/z = 1001.8877); found m/z = 1001.8740. Elemental Anal. Calc. for $C_{68}H_{108}Mo_2N_4O_4P_2S_8$: C, 52.49; H, 7.00; N, 3.60. Found: C, 52.53; H, 7.02; N, 3.54%.

^{13}C{^{1}H} NMR of Ph$_3$PS in CDCl$_3$-d$_1$. δ, ppm: 132.99 (d,^1J(P−C_i), 85.85 Hz), 132.35 (d,^3J(P−C_m), 11.11 Hz), 131.65 (d,^4J(P−C_p), 3.03 Hz), 128.61 (d,^2J(P−C_o), 12.12 Hz).

https://doi.org/10.1021/acs.inorgchem.4c05188
Inorg. Chem. 2025, 64, 4431−4446

Catalytic Experiments. The progress of the catalytic sulfur atom transfer reactions was monitored by ^{1}H NMR spectroscopy. Samples were prepared aerobically by mixing episulfide and deuterated solvent in a screw-capped NMR tube. A blank spectrum of the episulfide was obtained prior to the addition of **3** or **4a** at ambient temperature and pressure. Control reactions, under the same conditions without a catalyst, showed no identifiable alkene formation over the time of the catalytic runs. The predetermined molar ratio of episulfide (CS, SS, or PS) to **3** was mixed in an NMR tube with solvent ($CDCl_3$, CD_2Cl_2, etc.) to yield solutions that were 3, 1, 0.5, and 0.1 mol % in **3**. The NMR tube was wrapped with parafilm, and NMR spectra were recorded at regular intervals. For reactions including PPh_3, both ^{1}H NMR and $^{31}P\{^1H\}$ NMR spectra were collected. The alkene concentration was calculated based on the integration of the unreacted episulfide using the solvent signal as standard for the ^{1}H NMR spectrum, and for $^{31}P\{^1H\}$ NMR, PPh_4Br was used as an internal standard for integration. Sulfur that precipitated in the NMR tube was confirmed by melting point determination of 107−110 °C, and the solution mixture was analyzed by mass spectrum for experiments of CS with **3**, and with **3** and PPh_3 as indicated in the main text.

X-ray Crystallography. X-ray quality single crystals of K[**2**], were obtained by diffusion of dioxane/ether (1:1) mixture into a THF solution. Single crystals of **4a** were obtained by slow evaporation of a saturated solution in acetonitrile. The crystals of **4a** were isolated from their mother liquor, immediately immersed in cryogenic oil, and mounted. The X-ray single-crystal data were collected using MoKα radiation (λ = 0.71073 Å) on a Bruker D8Venture (Photon100 CMOS detector) diffractometer equipped with a Cryostream (Oxford Cryosystems) open-flow nitrogen cryostats at 295(2) K for **2** and 150(2) K for **4a**. The unit cell determination, data collection, data reduction, structure solution/refinement, and empirical absorption correction (SADABS) were carried out using Apex-III.[94] The structure was solved by direct method and refined by full-matrix least-squares in F2 for all data using SHELXTL and Olex2 software.[95−97] All nondisordered non-hydrogen atoms were refined anisotropically, and the hydrogen atoms were placed in the calculated positions and refined in the riding model.

■ ASSOCIATED CONTENT

Supporting Information

The Supporting Information is available free of charge at https://pubs.acs.org/doi/10.1021/acs.inorgchem.4c05188.

Crystallographic data summary, spectroscopic data for compounds, examples of spectroscopy for catalytic reactions, and additional relevant data (PDF)

Accession Codes

Deposition Numbers 2324144−2324145 contain the supplementary crystallographic data for this paper. These data can be obtained free of charge via the joint Cambridge Crystallographic Data Centre (CCDC) and Fachinformationszentrum Karlsruhe Access Structures service.

■ AUTHOR INFORMATION

Corresponding Author

Sigridur G. Suman − *Science Institute, University of Iceland, 107 Reykjavik, Iceland;* orcid.org/0000-0003-4283-6140; Email: sgsuman@hi.is

Authors

Dmitrii Razinkov − *Science Institute, University of Iceland, 107 Reykjavik, Iceland*

Ágúst Kvaran − *Science Institute, University of Iceland, 107 Reykjavik, Iceland*

Sigridur Jonsdottir − *Science Institute, University of Iceland, 107 Reykjavik, Iceland*

Complete contact information is available at: https://pubs.acs.org/10.1021/acs.inorgchem.4c05188

Author Contributions

All authors have given approval to the final version of the manuscript.

Notes

The authors declare no competing financial interest.

■ ACKNOWLEDGMENTS

Financial support by The Icelandic Centre of Research Project grant number 173667 and by the Technology Development Fund grant number. 2422618 are gratefully acknowledged. We thank Prof. Krishna K. Damodaran, the Department of Chemistry, University of Iceland, for the single crystal X-ray analysis of **2** and the data collection of **4a**. Icelandic Centre of Research Infrastructure grants numbers 150998, 210696, and 210521 are acknowledged for the purchase of single crystal X-ray diffractometer, FTIR, and UV−vis instruments.

■ REFERENCES

(1) Gellman, A. J.; Bussell, M. E.; Somorjai, G. A. Catalytic Hydrodesulfurization over the Mo(100) Single Crystal Surface. *J. Catal.* **1987**, *107*, 103−113.

(2) Kuwata, S.; Hidai, M. Hydrosulfido complexes of transition metals. *Coord. Chem. Rev.* **2001**, *213*, 211−305.

(3) Startsev, A. N. Concept of acid−base catalysis by metal sulfides. *Catal. Today* **2009**, *144* (3), 350−357.

(4) Coucouvanis, D. Use of preassembled iron/sulfur and iron/molybdenum/sulfur clusters in the stepwise synthesis of potential analogs for the Fe/Mo/S site in nitrogenase. *Acc. Chem. Res.* **1991**, *24* (1), 1−8.

(5) Shearer, J.; Kung, I. Y.; Lovell, S.; Kovacs, J. A. A Co(III) Complex in a Mixed Sulfur/Nitrogen Ligand Environment: Modeling the Substrate- and Product-Bound Forms of the Metalloenzyme Thiocyanate Hydrolase. *Inorg. Chem.* **2000**, *39* (22), 4998−4999.

(6) Yano, T.; Wasada-Tsutsui, Y.; Ikeda, T.; Shibayama, T.; Kajita, Y.; Inomata, T.; Funahashi, Y.; Ozawa, T.; Masuda, H. Co(III) Complexes with N2S3-Type Ligands as Structural/Functional Models for the Isocyanide Hydrolysis Reaction Catalyzed by Nitrile Hydratase. *Inorg. Chem.* **2018**, *57* (8), 4277−4290.

(7) Johnson-Winters, K.; Tollin, G.; Enemark, J. H. Elucidating the catalytic mechanism of sulfite oxidizing enzymes using structural, spectroscopic, and kinetic analyses. *Biochemistry* **2010**, *49* (34), 7242−7254.

(8) Stiefel, E. I. Chemical Keys to Molybdenum Enzymes. *J. Chem. Soc., Dalton Trans.* **1997**, 3915−3923.

(9) Stiefel, E. I. Transition Metal Sulfur Chemistry: Biological and Industrial Significance and Key Trends. In *Transition Metal Sulfur Chemistry*, ACS Symposium Series; ACS Publications, 1996; 2−38.

(10) Rakowski Dubois, M. Catalytic Applications of Transition-Metal Complexes with Sulfide Ligands. *Chem. Rev.* **1989**, *89* (1), 1−9.

(11) Young, C. G. Facets of early transition metal-sulfur chemistry: Metal-sulfur ligand redox, induced internal electron transfer, and the reactions of metal-sulfur complexes with alkynes. *J. Inorg. Biochem.* **2007**, *101* (11−12), 1562−1585.

(12) Liu, H.; Jiang, X. Transfer of Sulfur: From Simple to Diverse. *Chem. - Asian J.* **2013**, *8* (11), 2546−2563.

(13) Topsöe, H.; Clausen, B. S. Importance of Co-Mo-S Type Structures in Hydrodesulfurization. *Catal. Rev.* **2007**, *26* (3−4), 395−420.

(14) Adam, W.; Bargon, R. M. Synthesis of Thiiranes by Direct Sulfur Transfer: The Challenge of Developing Effective Sulfur Donors and Metal Catalysts. *Chem. Rev.* **2004**, *104* (1), 251−262.

(15) Pétillon, F. Y.; Schollhammer, P.; Talarmin, J. Recent advances in the chemistry of tris(thiolato) bridged cyclopentadienyl dimolybdenum complexes. *Coord. Chem. Rev.* **2017**, *331*, 73−92.

(16) Ooi, M. L.; Lim, C. E.; Wong, R. C. S.; Ng, S. W. Isolation and characterization of thiolato complexes of [CpCr(SBz)]2S, isomeric trans [CpMo(CO)(SBz)]2 and [CpMo(SBz)2]2 (Cp = (η5-C5H5), Bz = PhCH2) from the reactivity of bibenzyl disulfide towards [CpM(CO)3]2 (M = Cr, Mo). *Inorg. Chim. Acta* **2017**, *467*, 364−371.
(17) Farrell, W. S.; Zavalij, P. Y.; Sita, L. R. Catalytic Production of Isothiocyanates via a Mo(II)/Mo(IV) Cycle for the "Soft" Sulfur Oxidation of Isonitriles. *Organometallics* **2016**, *35* (14), 2361−2366.
(18) Garrett, B. R.; Polen, S. M.; Click, K. A.; He, M.; Huang, Z.; Hadad, C. M.; Wu, Y. Tunable Molecular MoS2 Edge-Site Mimics for Catalytic Hydrogen Production. *Inorg. Chem.* **2016**, *55* (8), 3960−3966.
(19) Adam, W.; Bargon, R. M.; Schenk, W. A. Direct Episulfidation of Alkenes and Allenes with Elemental Sulfur and Thiiranes as Sulfur Sources, Catalyzed by Molybdenum Oxo Complexes. *J. Am. Chem. Soc.* **2003**, *125* (13), 3871−3876.
(20) Adam, W.; Bargon, R. M.; Bosio, S. G.; Schenk, W. A.; Stalke, D. Direct Synthesis of Isothiocyanates from Isonitriles by Molybdenum-Catalyzed Sulfur Transfer with Elemental Sulfur. *J. Org. Chem.* **2002**, *67* (20), 7037−7041.
(21) Rys, A. Z.; Harpp, D. N. Catalytic sulfuration of dienes with metallocene polysulfides. *Tetrahedron Lett.* **1998**, *39* (50), 9139−9142.
(22) Ward, J. P.; Lim, P. J.; Evans, D. J.; White, J. M.; Young, C. G. Tungsten Ligand-Based Sulfur-Atom-Transfer Catalysts: Synthesis, Characterization, Sustained Anaerobic Catalysis, and Mode of Aerial Deactivation. *Inorg. Chem.* **2020**, *59* (23), 16824−16828.
(23) Sugimoto, H.; Tajima, R.; Sakurai, T.; Ohi, H.; Miyake, H.; Itoh, S.; Tsukube, H. Reversible Sulfurization−Desulfurization of Tungsten Bis(dithiolene) Complexes. *Angew. Chem., Int. Ed.* **2006**, *45* (21), 3520−3522.
(24) Eagle, A. A.; Gable, R. W.; Thomas, S.; Sproules, S. A.; Young, C. G. Sulfur atom transfer reactions of tungsten(VI) and tungsten(IV) chalcogenide complexes. *Polyhedron* **2004**, *23* (2), 385−394.
(25) Wang, J.-J.; Kryatova, O. P.; Rybak-Akimova, E. V.; Holm, R. H. Comparative Kinetics and Mechanism of Oxygen and Sulfur Atom Transfer Reactions Mediated by Bis(dithiolene) Complexes of Molybdenum and Tungsten. *Inorg. Chem.* **2004**, *43* (25), 8092−8101.
(26) Ibdah, A.; Jenks, W. S.; Espenson, J. H. Kinetics, Mechanism, and Computational Studies of Rhenium-Catalyzed Desulfurization Reactions of Thiiranes (Thioepoxides). *Inorg. Chem.* **2006**, *45* (14), 5351−5357.
(27) Arisawa, M.; Yamaguchi, M. Rhodium-Catalyzed Synthesis of Organosulfur Compounds Involving S-S Bond Cleavage of Disulfides and Sulfur. *Molecules* **2020**, *25* (16), 3595.
(28) Arisawa, M.; Ichikawa, T.; Yamaguchi, M. Synthesis of thiiranes by rhodium-catalyzed sulfur addition reaction to reactive alkenes. *Chem. Commun.* **2015**, *51* (42), 8821−8824.
(29) Arisawa, M.; Tanaka, K.; Yamaguchi, M. Rhodium-catalyzed sulfur atom exchange reaction between organic polysulfides and sulfur. *Tetrahedron Lett.* **2005**, *46* (28), 4797−4800.
(30) Moon, S.; Kato, M.; Nishii, Y.; Miura, M. Synthesis of Benzo[b]thiophenes through Rhodium-Catalyzed Three-Component Reaction using Elemental Sulfur. *Adv. Synth. Catal.* **2020**, *362* (8), 1669−1673.
(31) Donahue, J. P. Thermodynamic Scales for Sulfur Atom Transfer and Oxo-for-Sulfido Exchange Reactions. *Chem. Rev.* **2006**, *106*, 4747−4783.
(32) Huang, C. Y.; Doyle, A. G. The chemistry of transition metals with three-membered ring heterocycles. *Chem. Rev.* **2014**, *114* (16), 8153−8198.
(33) Dave, M.; Rajagopal, A.; Damm-Ruttensperger, M.; Schwarz, B.; Nägele, F.; Daccache, L.; Fantauzzi, D.; Jacob, T.; Streb, C. Understanding homogeneous hydrogen evolution reactivity and deactivation pathways of molecular molybdenum sulfide catalysts. *Sustainable Energy Fuels* **2018**, *2* (5), 1020−1026.
(34) Coucouvanis, D. Syntheses, Structures, and Reactions of Binary and Tertiary Thiomolybdate Complexes Containing the (O)Mo(Sx) AND (S)Mo(Sx) Functional Groups (x = 1, 2, 4). In *Advances in Inorganic Chemistry*, Sykes, A. G., Ed.; Academic Press, *45*; 1998; 1−73.
(35) Jacob, J.; Espenson, J. H. Stereospecific rhenium catalyzed desulfurization of thiiranes. *Chem. Commun.* **1999**, *11*, 1003−1004.
(36) Koshino, N.; Espenson, J. H. Kinetics and Mechanism of Oxygen Atom Transfer from Methyl Phenyl Sulfoxide to Triarylphosphines Catalyzed by an Oxorhenium(V) Dimer. *Inorg. Chem.* **2003**, *42* (18), 5735−5742.
(37) Sorsche, D.; Miehlich, M. E.; Zolnhofer, E. M.; Carroll, P. J.; Meyer, K.; Mindiola, D. J. Metal−Ligand Cooperativity Promoting Sulfur Atom Transfer in Ferrous Complexes and Isolation of a Sulfurmethylenephosphorane Adduct. *Inorg. Chem.* **2018**, *57* (18), 11552−11559.
(38) Young, C. G.; Laughlin, L. J.; Colmanet, S.; Scrofani, S. D. B. Oxygen Atom Transfer, Sulfur Atom Transfer, and Correlated Electron−Nucleophile Transfer Reactions of Oxo- and Thiomolybdenum(IV) Complexes: Synthesis of Oxothiomolybdenum(VI) and (Hydroxo)oxomolybdenum(V) Species. *Inorg. Chem.* **1996**, *35* (18), 5368−5377.
(39) Maiti, D.; Woertink, J. S.; Vance, M. A.; Milligan, A. E.; Narducci Sarjean, A. A.; Solomon, E. I.; Karlin, K. D. Copper(I)/S8 Reversible Reactions Leading to an End-On Bound Dicopper(II) Disulfide Complex: Nucleophilic Reactivity and Analogies to Copper-Dioxygen Chemistry. *J. Am. Chem. Soc.* **2007**, *129*, 8882−8892.
(40) Ólafsson, S. N.; Kvaran, Á.; Jonsdottir, S.; Suman, S. G. Non-rigid coordination behavior of the ambidentate phosphinoyldithioformate ligands, [S2CP(O)R2]-, (R = Ph, CH2Ph) in organometallic Lead(IV) and Mercury(II) compounds. *J. Organomet. Chem.* **2018**, *854*, 38−48.
(41) Ólafsson, S. N.; Bjornsson, R.; Helgason, Ö.; Jonsdottir, S.; Suman, S. G. Coordination geometry determination of stannane compounds with phosphinoyldithioformate ligands using multinuclear NMR, Sn Mössbauer and DFT methods. *J. Organomet. Chem.* **2016**, *825*−*826*, 125−138.
(42) Ólafsson, S. N.; Flensburg, C.; Andersen, P. Lead(IV) complexes with phosphinoyldithioformates, R2P(O)CS2, (R = Ph or PhCH2). Syntheses and characterization. Crystal structures of PPh4[S2CP(O)Ph2]-0.5H2O, [PbPh2{S2CP(O)Ph2}2] and [PbPh2Cl{S2CP(O)Ph2}]. *J. Chem. Soc., Dalton Trans.* **2000**, No. 23, 4360−4368.
(43) Razinkov, D.; Ingvarsdottir, H. I.; Kvaran, Á.; Jonsdottir, S.; Suman, S. G. Coordination Properties of Non-Rigid Phosphinoyldithioformate Complexes of the [Mo2O2(μ-S)2]2+ Cation in Catalytic Sulfur Transfer Reactions with Thiiranes. *Catalysts* **2021**, *11*, 593−611.
(44) Yoo, B. W.; Kim, J. Y. Selective and efficient desulfurization of thiiranes with Mo(CO)6. *J. Sulfur Chem.* **2020**, *41* (1), 13−18.
(45) Ogienko, D. S.; Smolentsev, A. I.; Bashirov, D. A.; Afonin, M. Y.; Petrov, P. A.; Konchenko, S. N. Syntheses and structures of complexes {Mo2S2O2}2+ with labile Cl−and DMF ligands. *Russ. J. Coord. Chem.* **2015**, *41* (11), 759−764.
(46) Ólafsson, S. N.; Petersen, T. N.; Andersen, P. Crystal structure of diphenylbis(diphenyldithio-phosphinato)lead(IV), PbPh2-(S2PPh2)2. *Acta Chem. Scand.* **1996**, *50* (9), 745−748.
(47) Gusarova, N. K.; Malysheva, S. F.; Kuimov, V. A.; Belogorlova, N. A.; Mikhailenko, V. L.; Trofimov, B. A. Nucleophilic additon of phosphine to 1-(tert-butyl)-4-vinylbenzene: a short-cut to bulky secondary and tertiary phosphines and their chalcogenides. *Mendeleev Commun.* **2008**, *18* (5), 260−261.
(48) Gusarova, N. K.; Arbuzova, S. N.; Trofimov, B. A. Novel general halogen-free methodology for the synthesis of organophosphorus compounds. *Pure Appl. Chem.* **2012**, *84* (3), 439−459.
(49) Bondi, A. Van der Waals Volume and Radii. *J. Phys. Chem.* **1964**, *68*, 441−451.
(50) Shihada, A. F.; Weller, F. Syntheses, spectroscopic studies, and crystal structures of Me2Sn(O2PPh2)2, Ph2Pb(O2PMe2)2, and Ph2Pb(O2PPh2)2. *Z. Anorg. Allg. Chem.* **2001**, *627* (4), 638−644.

https://doi.org/10.1021/acs.inorgchem.4c05188
Inorg. Chem. 2025, 64, 4431−4446

(51) Balogová, M.; Sharma, S.; Cherek, P.; Ólafsson, S. N.; Jónsdóttir, S.; Ögmundsdóttir, H. M.; Damodaran, K. K. Cytotoxic effects of halogenated tin phosphinoyldithioformate complexes against several cancer cell lines. *Dalton Trans.* **2022**, *51* (34), 13119−13128.
(52) Bandoli, G.; Bortolozzo, G.; Clemente, D. A.; Croatto, U.; Panattoni, C. Crystal and molecular structure of triphenylphosphine oxide. *J. Chem. Soc. A* **1970**, *0*, 2778−2780.
(53) Al-Farhan, K. A. Crystal structure of triphenylphosphine oxide. *J. Crystallogr. Spectrosc. Res.* **1992**, *22* (6), 687−689.
(54) Fenske, D.; Mattes, R.; Löns, J.; Tebbe, K. F. Die Kristallstruktur von Diphenylphosphinsäure. *Chem. Ber.* **1973**, *106* (4), 1139−1144.
(55) Gushchin, A. L.; Laricheva, Y. L.; Alferova, N. I.; Virovets, A. V.; Sokolov, M. N. Binuclear cluster complexes of molybdenum containing 2,2′-bipyridine and 1,10-phenanthroline: Synthesis and structure. *J. Struct. Chem.* **2013**, *54* (4), 752−758.
(56) Coucouvanis, D.; Toupadakis, A.; Lane, J. D.; Koo, S. M.; Kim, C. G.; Hadjikyriacou, A. Reactivity of the Mo(O)(S) functional group in the [(L)Mo(O)(μ-S)2Mo(O)(S)]n- dimeric thiomolybdate complexes, (L = C5H5—, n = 1; S42-, n = 2) and implications regarding the function of xanthine oxidase. Synthesis and structural characterization of [(DMF)3Mo(O)(μ-S)2Mo(O)(S2)], [Ph4P]-[(C5H5)Mo(O)(μ-S)2Mo(O)(S2)], [Ph4P]2[(S4)Mo(O)(μ-S)-2Mo(O)(S)] and (Et4N)4{[(S4)Mo(O)(μ-S)2Mo(O)(S)]2}. *J. Am. Chem. Soc.* **1991**, *113* (14), 5271−5282.
(57) Müller, A. Coordination chemistry of Mo- and W-S compounds and some aspects of hydrodesulfurization catalysis. *Polyhedron* **1986**, *5* (1), 323−340.
(58) Gabay, J.; Dietz, S.; Bernatis, P.; DuBois, M. R. Dinuclear cyclopentadienylmolybdenum complexes containing thioether ligands. Ligand substitution and desulfurization reactions. *Organometallics* **1993**, *12* (9), 3630−3635.
(59) Recatalá, D.; Gushchin, A. L.; Llusar, R.; Galindo, F.; Brylev, K. A.; Ryzhikov, M. R.; Kitamura, N. Dithiolene dimetallic molybdenum-(v) complexes displaying intraligand charge transfer (ILCT) emission. *Dalton Trans.* **2013**, *42* (36), 12947−12955.
(60) Suman, S. G.; Snæbjörnsson, T.; Ragnarsdóttir, O.; Polukeev, A. V.; Wendt, O. F. Synthesis of mixed salts of the [Mo2O2(μ-S)2(SCN)6-n(L)n](4+n)−anion (n = 0−2); structures of [Mo2O2-(μ-S)2(SCN)5(CH3CN)]3−, [Mo2O2(μ-S)2(CN)5]3−, and [Mo2O2(μ-S)2(CN)2(O)]2−, and probing the ligand exchange of thiocyanate and cyanide. *Polyhedron* **2021**, *209*, No. 115447.
(61) Birgisson, B. O.; Monger, L. J.; Damodaran, K. K.; Suman, S. G. Synthesis and characterization of asymmetric [Mo2O2(μ-S)2(S2)-(L)] complexes (L = bipy, en, dien) and their heterogeneous reaction with propylene sulfide. *Inorg. Chim. Acta* **2020**, *501*, No. 119272.
(62) Suman, S. G.; Gretarsdottir, J. M.; Penwell, P. E.; Gunnarsson, J. P.; Frostason, S.; Jonsdottir, S.; Damodaran, K. K.; Hirschon, A. Reaction Chemistry of the syn-[Mo2O2(μ-S)2(S2)(DMF)3] Complex with Cyanide and Catalytic Thiocyanate Formation. *Inorg. Chem.* **2020**, *59* (11), 7644−7656.
(63) Djordjevic, C.; Vuletic, N.; Jacobs, B. A.; Lee-Renslo, M.; Sinn, E. Molybdenum(VI) Peroxo α-Amino Acid Complexes: Synthesis, Spectra, and Properties of MoO(O2)2(α-aa)(H2O) for α-aa = Glycine, Alanine, Proline, Valine, Leucine, Serine, Asparagine, Glutamine, and Glutamic Acid. X-ray Crystal Structures of the Glycine, Alanine, and Proline Compounds. *Inorg. Chem.* **1997**, *36* (9), 1798−1805.
(64) Yoshida, R.; Ogasahara, S.; Akashi, H.; Shibahara, T. Crystal structural diversity of sulfur-bridged cysteinato dimolybdenum(V)-complexes: The influence of counter metal cations. *Inorg. Chim. Acta* **2012**, *383*, 157−163.
(65) Cotton, F. A.; Wing, R. M. The Crystal and Molecular Structure of cis-(Diethylenetriamine)molybdenum Tricarbonyl; the Dependence of Mo-C Bond Length on Bond Order. *Inorg. Chem.* **1965**, *4* (3), 314−317.
(66) Blake, A. B.; Cotton, F. A.; Wood, J. S. The Crystal, Molecular, and Electronic Structures of a Binuclear Oxomolybdenum(V) Xanthate Complex. *J. Am. Chem. Soc.* **1964**, *86* (15), 3024−3031.
(67) Clegg, W.; Mohan, N.; Mueller, A.; Neumann, A.; Rittner, W.; Sheldrick, G. M. Crystal and molecular structure of [N(CH3)4]2-[Mo2O2S2(S2)2]: a compound with two S22- ligands. *Inorg. Chem.* **1980**, *19* (7), 2066−2069.
(68) Albright, T. A.; Freeman, W. J.; Schweizer, E. E. Nuclear magnetic resonance studies. IV. Carbon and phosphorus nuclear magnetic resonance of phosphine oxides and related compounds. *J. Org. Chem.* **1975**, *40* (23), 3437−3441.
(69) Grim, S. O.; Briggs, W. L.; Barth, R. C.; Tolman, C. A.; Jesson, J. P. Unsymmetrical bis-phosphorus ligands. IV. Group VI metal carbonyl derivatives of diphenylphosphinomethyl and diphenylphosphinomethyl phosphinites, (C6H5)2P(CH2)nOP(C6H5)2, n = 1 or 2, and an unusual phosphorus chemical shift chelate effect. *Inorg. Chem.* **1974**, *13* (5), 1095−1100.
(70) Birnbaum, J.; Laurie, J. C. V.; DuBois, M. R. Insertions of unactivated olefins into the hydrosulfido ligand of a cationic cyclopentadienylmolybdenum complex. *Organometallics* **1990**, *9* (1), 156−164.
(71) Arterburn, J. B.; Perry, M. C. Rhenium catalyzed sulfurization of phosphorus(III) compounds with thiiranes: New reagents for phosphorothioate ester synthesis. *Tetrahedron Lett.* **1997**, *38* (44), 7701−7704.
(72) Coffey, T. A.; Hogarth, G. Synthesis and structure of [Mo2(NR)2(η2-S2CNEt2)2(μ-S)(μ-η2-η2-S2)] (R = 2,6-Pr2iC6H3): a molecular model for molybdenum trisulphide? *Polyhedron* **1997**, *16* (1), 165−169.
(73) Klingelhöfer, P.; Müller, U. Synthese und Struktur des μ-Sulfido-μ-disulfido-octabromodiwolframat(V)-Ions [W2S3Br8]2−. *Z. Anorg. Allg. Chem.* **1986**, *542* (11), 7−12.
(74) Newton, W. E.; McDonald, J. W.; Yamanouchi, K.; Enemark, J. H. Synthesis and molecular structure of molybdenum(V) dimers with mixed oxo and sulfido terminal ligands: removal of terminal sulfide by triphenylphosphine and cyanide. *Inorg. Chem.* **1979**, *18* (6), 1621−1626.
(75) Kubas, G. J.; Jarvinen, G. D.; Ryan, R. R. Stereochemical and electronic control of M-SO2 bonding geometry in d6 molybdenum and tungsten sulfur dioxide complexes: novel.eta.1.tautm. .eta.2 sulfur dioxide linkage isomerization in Mo(CO)2(PPh3)2(CNR)(SO2) and structures of Mo(CO)3(P-iso-Pr3)2(SO2) and [Mo(CO)2(py)-(PPh3)(.mu.-SO2)]2. *J. Am. Chem. Soc.* **1983**, *105* (7), 1883−1891.
(76) Bose, M.; Moula, G.; Begum, A.; Sarkar, S. Synthesis and characterization of cyano and isocyano complexes of bis(dithiolato) molybdenum using Me3SiCN: a route to a cyanide-bridged multimer to a monomer. *New J. Chem.* **2018**, *42* (7), 5580−5592.
(77) Zhang, Y.; Hanna, B. S.; Dineen, A.; Williard, P. G.; Bernskoetter, W. H. Functionalization of Carbon Dioxide with Ethylene at Molybdenum Hydride Complexes. *Organometallics* **2013**, *32* (14), 3969−3979.
(78) Doonan, C. J.; Gourlay, C.; Nielsen, D. J.; Ng, V. W.; Smith, P. D.; Evans, D. J.; George, G. N.; White, J. M.; Young, C. G. d(1) Oxosulfido-Mo(V) Compounds: First Isolation and Unambiguous Characterization of an Extended Series. *Inorg. Chem.* **2015**, *54* (13), 6386−6396.
(79) Crawford, A. M.; Cotelesage, J. J. H.; Prince, R. C.; George, G. N. The Catalytic Mechanisms of the Molybdenum and Tungsten Enzymes. In *Metallocofactors that Activate Small Molecules: Structure and Bonding*, Ribbe, M. W., Ed.; Springer International Publishing, *179*; 2019; 63−100.
(80) Gushchin, A. L.; Laricheva, Y. A.; Sokolov, M. N.; Llusar, R. Tri- and tetranuclear molybdenum and tungsten chalcogenide clusters: on the way to new materials and catalysts. *Russ. Chem. Rev.* **2018**, *87* (7), 670−706.
(81) Montilla, F.; Galindo, A. Oxidodiperoxidomolybdenum Complexes: Properties and Their Use as Catalysts in Green Oxidations. In *Reference Module in Chemistry, Molecular Sciences and Chemical Engineering*; Elsevier, 2017.

https://doi.org/10.1021/acs.inorgchem.4c05188
Inorg. Chem. 2025, 64, 4431−4446

(82) Sproules, S.; Eagle, A. A.; George, G. N.; White, J. M.; Young, C. G. Mononuclear Sulfido-Tungsten(V) Complexes: Completing the Tp*MEXY (M = Mo, W; E = O, S) Series. *Inorg. Chem.* **2017**, *56* (9), 5189−5202.
(83) Denney, D. B.; Boskin, M. J. Concerning the Mechanism of the Reaction of Trisubstituted Phosphines with Episulfides1. *J. Am. Chem. Soc.* **1960**, *82* (17), 4736−4738.
(84) Monger, L. J.; Razinkov, D.; Bjornsson, R.; Suman, S. G. Synthesis, Characterization, and Reaction Studies of Pd(II) Tripeptide Complexes. *Molecules* **2021**, *26* (17), 5169.
(85) Gal, A. W.; Gosselink, J. W.; Vollenbroek, F. A. Rhodium(I) phosphine complexes containing bidentate unsaturated thio ligands. I. Synthesis and characterisation. *J. Organomet. Chem.* **1977**, *142* (3), 357−374.
(86) Hogarth, G.; Richards, I. Crystal and molecular structures of syn and anti isomers of [MoO(μ-NAr)(S2CNR2)]2 (R = Et, Pr; Ar = Ph, p-tolyl). *Inorg. Chim. Acta* **2005**, *358* (3), 707−712.
(87) Döring, A.; Schulzke, C.; Zhang, Q. Synthesis, characterization and structural analysis of isostructural dinuclear molybdenum and tungsten oxo-bis-μ-sulfido-benzenedithiolene complexes. *Inorg. Chim. Acta* **2010**, *363* (14), 4140−4144.
(88) Cagle, E. C.; Totsch, T. R.; Erdmann, M. A.; Gray, G. M. A 31P{1H} NMR Spectroscopic Study of Phosphorus-Donor Ligands and Their Transition Metal Complexes. *J. Chem. Educ.* **2018**, *95* (6), 1054−1059.
(89) Ojo, W.-S.; Pétillon, F. Y.; Schollhammer, P.; Talarmin, J. Carbon−Sulfur and Carbon−Halogen Bond Cleavage of Acyclic or Cyclic Thioethers, Thiophenes, and Dihaloalkanes with the Trithiolato-Bridged Cation [Mo2Cp2(μ-SMe)3(MeCN)2]+. *Organometallics* **2010**, *29* (2), 448−462.
(90) Müller, A.; Diemann, E. Polysulfide Complexes of Metals. In *Advances in Inorganic Chemistry*, Emeléus, H. J.; Sharpe, A. G., Eds.; Academic Press, *31*; 1987; 89−122.
(91) Razinkov, D.; Agostinho, B.; Suman, S. G.; Sousa, A. F. Leveraging molybdenum sulfur compounds as catalysts for the synthesis of biobased poly(ethylene 2,5-furandicarboxylate) and recycling. *RSC Sustain* **2025**, *3*, 323−330.
(92) Kobler, H.; Munz, R.; Gasser, A. G.; Simchen, G. A Simple Synthesis of Tetraalkyammonium Salts with Functional Anions. *Chemischer Informationsdienst* **1979**, *10*14. .
(93) Kobler, H.; Munz, R.; Gasser, G. A.; Simchen, G. Eine einfache Synthese von Tetraalkylammoniumsalzen mit funktionellen Anionen. *Justus Liebigs Ann. Chem.* **1978**, *1978* (12), 1937−1945.
(94) *Apex III*; Bruker AXS Inc.: Madison, WI, USA, 2015. (accessed 2015).
(95) Dolomanov, O. V.; Bourhis, L. J.; Gildea, R. J.; Howard, J. A. K.; Puschmann, H. OLEX2: a complete structure solution, refinement and analysis program. *J. Appl. Crystallogr.* **2009**, *42* (2), 339−341.
(96) Sheldrick, G. M. Crystal structure refinement with SHELXL. *Acta Crystallogr., Sect. C: Struct. Chem.* **2015**, *71* (Pt 1), 3−8.
(97) Bourhis, L. J.; Dolomanov, O. V.; Gildea, R. J.; Howard, J. A. K.; Puschmann, H. The anatomy of a comprehensive constrained, restrained refinement program for the modern computing environment - Olex2 dissected. *Acta Crystallogr., Sect. A: Found. Adv.* **2015**, *71* (1), 59−75.

https://doi.org/10.1021/acs.inorgchem.4c05188
Inorg. Chem. 2025, 64, 4431−4446